Advanced process control for power plants

Improving overall performance through control of internal process variables

J. Marcus Blaazer

Master of Science Thesis

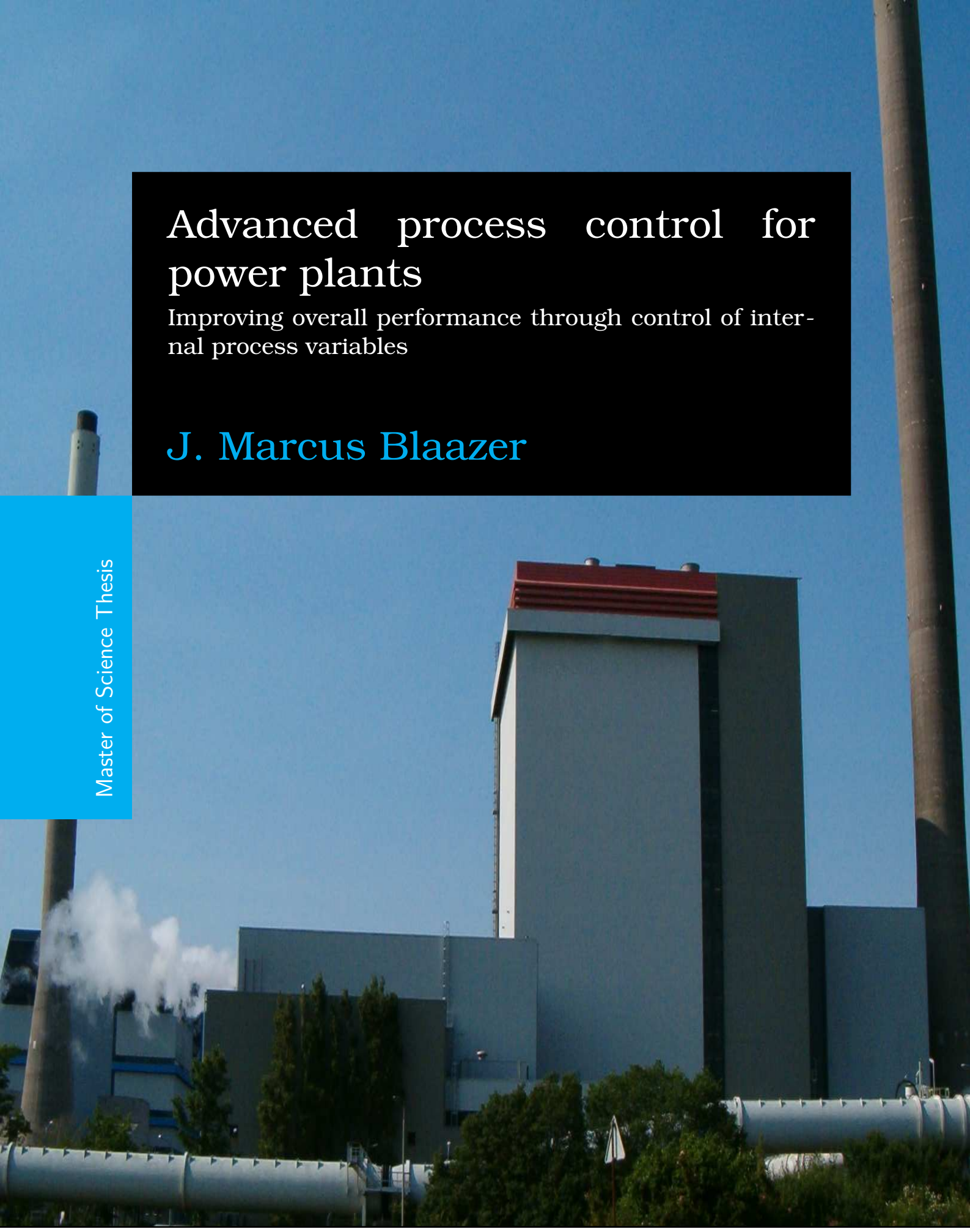

TU Delft Delft University of Technology

Delft Center for Systems and Control

Advanced process control for power plants

Improving overall performance through control of internal process variables

Master of Science Thesis

For the degree of Master of Science in Systems and Control at Delft University of Technology

J. Marcus Blaazer

August 17, 2010

Faculty of Mechanical, Maritime and Materials Engineering (3mE) · Delft University of Technology

The work in this thesis was supported by Laborelec (Linkebeek, Belgium). Their cooperation is hereby gratefully acknowledged.

Abstract

The European power market has changed substantially over the past twenty years. Increased competition, increasing use of renewables and environmental regulations contributed to a power market in which the power supply and demand fluctuates more frequently than ever. By nature, most power plants are sensitive to these fluctuations. The main reason for this is coupling between throughput (i.e. power output) and quality (e.g. pressure, temperature) and coupling amongst the quality parameters itself. As a consequence, when throughput fluctuates the quality is disturbed and oscillations occur in many of the process loops. Since these oscillations reduce power plant efficiency, increase wear and reduce plant lifetime it is desired to investigate solutions.

In this study the effect of multivariable advanced process control (MIMO APC) on internal process loop oscillation and performance is investigated. Furthermore, the effect of improved process loop control on overall power plant performance is studied.

To this end, a conventional drum-boiler power plant simulator (PID-controlled) is equipped with an H_∞-controller. A safe shutdown master-slave control structure is proposed to enable practical implementation. To accentuate the influence of improved internal process loop control on overall performance, the H_∞-controller will be responsible for four boiler process loops (the boiler has a central role in determining the overall behavior of power plants).

This study shows that MIMO APC is a viable method for reducing oscillations and improving performance of internal process loops. It has become clear that better internal control also improves overall power plant performance. As a result, the effective maximum power production rate can be increased, which was found to have a surprisingly small effect on the achieved performance increase. These results indicate that it is possible to increase the economic potential of power plants using MIMO APC.

Table of Contents

List of Figures

List of Tables

Acknowledgements

The current thesis on Advanced Process Control for Power Plants was conducted to obtain the M.Sc. degree in Control Engineering at the faculty of Mechanical, Maritime and Materials Engineering, Delft University of Technology (TU Delft). This research was supported by Laborelec (Linkebeek, Belgium) and the Delft Center for Systems and Control (DCSC) at TU Delft. I would like to thank both parties for giving me this opportunity.

I would like to thank my supervisors at Laborelec, Ir. T. Museur and Dr. Ir. B. Codrons for their support during this project and their thoughts and advice afterwards.

At TU Delft, Dr.Ir. X.J.A. Bombois and Ir. A.E.M. Huesman are gratefully acknowledged for supervising my work. During this study your guidance and assistance was of great support. Furthermore, I want to thank MSc. C. Trapp (dpt. Process & Energy, TU Delft) for reading this thesis. Finally I want to thank Prof. Dr. Ir. P.M.J. Van den Hof for taking this project under his care.

Next to the support of Laborelec and DCSC, I would like to thank my family and friends. You gave me support and advice when I requested it, but you also gave me motivation when I needed it. Of this group, I especially want to mention Ir. K. Hoetmer, A. R. Blaazer M.Sc., Drs. Ir. J.G. Blaazer and E. Jansen B.Sc. for reading this work several times combined with your invaluable advice.

Delft, University of Technology — J. Marcus Blaazer
August 17, 2010

This thesis is dedicated to Ir. A. Mulder † (former Chief of Production and Operation at Provinciaal Elektriciteitsbedrijf Noord-Holland) for giving me the motivation and energy to conduct this research as good as possible.

Chapter 1

Introduction

This chapter provides a general introduction to this study. Starting with multiple input multiple output (MIMO) advanced process control (APC) for power plants (Section 1-1), placing focus on reduction of oscillations in vital process variables (Section 1-2). Hereafter the aim of the investigation is described (Section 1-3), followed by the applied methods (Section 1-4).

1-1 Advanced Process Control for Power Plants

The European power market has changed substantially over the past twenty years. Increased competition, increasing use of renewables (wind, solar and bio energy) and environmental regulations transformed the power market into a genuine trade market. As a result the supply of, and demand for, power fluctuates more frequently than ever [1].

Producing power in this kind of market is a substantial challenge for power plant operators since most power plants are by nature sensitive to fluctuations in power demand [2]. The reason for this is coupling in the power plant process. In power plants there is coupling between throughput (i.e. power output) and quality (e.g. pressure, temperature) and amongst the quality parameters itself. As a consequence, when throughput fluctuates the quality is disturbed. This is indicated by oscillations that occur in many quality parameters after throughput changes. Generally, it is desired to keep quality at a certain level independent of throughput. Oscillations reduce power plant efficiency, increase wear and reduce plant lifetime [2].

Power plant operators have four options to adapt to the new conditions: building flexible types of power plants (gas turbine or combined cycle power plants), making power plants more flexible through design parameters (e.g. alternative materials, dimensions or fuel type), demand side management with storage capacity (smart grid) or improving the process control of individual power plants. All options are currently under investigation and are complementary. However, only power plant control system adaptation is currently available for power

plant operating companies. Furthermore, it is a solution for existing plants, while the other options are only viable for new systems [3].

On power plant level, control can reduce oscillations and their effects through decoupling and more effective multi-loop disturbance rejection [2, 4]. Decoupling of the process loops (i.e. quality parameters) prevents or decreases the propagation of disturbances through the power plant. Hence, fluctuations in throughput will influence a smaller part of the power plant. Furthermore throughput change acts as a disturbance on quality so its influence can be minimized through more effective multi-loop disturbance rejection. Unfortunately, this cannot be achieved by classical power plant control systems. These systems consist of multiple single input single output (SISO) PID controllers, which are not able to take control-loop interaction into account [5, 6].

It is known that the addition of a multivariable advanced process control system improves power plant control performance considerably [3]. MIMO APC can achieve decoupling. Furthermore, MIMO APC is a much more efficient method of oscillation reduction, because it regulates multiple process variables at once [4]. Nevertheless, in practice, power plant operators scarcely adopt MIMO APC because it reduces the possibility to manually operate single parts of the plant [2]. Therefore, it is proposed to use a control structure in which MIMO APC corrects the classical control system. In this way, whenever requested by the operator, the APC can be disconnected while the classical control system remains operational.

This study will focus on the control of the boiler system because of its central role in determining the overall behavior of the power plant [3]. Previous research by Laborelec showed that MIMO APC can reduce the oscillations in the feedwater system, a boiler sub-system, significantly [7]. Therefore as a next step towards plant-wide MIMO APC, the whole boiler will be included in MIMO APC. This will be achieved through considering the steam conditions at the boiler outlet (pressure and temperature) and the feedwater system. In this study only drum-boilers are considered since most conventional power plants have this design [3].

1-2 Problem Description

To illustrate the central role of the boiler, a brief process description is given. Hereafter we focus on the boiler outlet conditions and the feedwater system. It will become clear how steam properties, at the boiler outlet, determine the power output of the power plant. Furthermore, it is shown how the feedwater system contributes to achieving the desired steam properties.

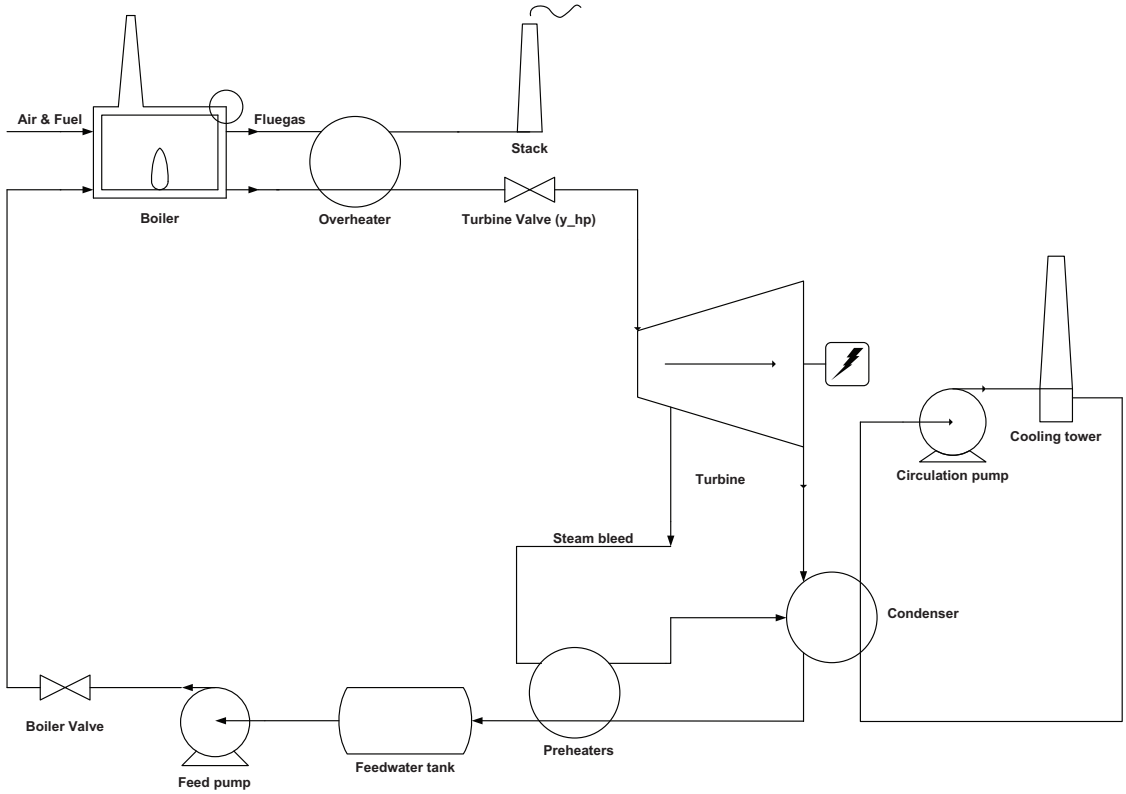

Figure 1-1: Process flow diagram of a power plant

In conventional drum-boiler power plants (Figure 1-1), power is produced by a steam turbine. This turbine drives the alternator. Steam is generated from water in a coal, oil, gas or biomass-fired boiler. Thereafter, steam is brought to the appropriate temperature and pressure conditions before being expanded in the turbine. After expansion, the condenser converts the remaining steam to water. The water is pre-heated and stored in the feedwater tank. Finally the variable speed feed pump draws the required amount of water from the tank, pressurizes it and feeds it to the boiler. The boiler valve adjusts the amount and pressure of the water that enters the boiler.

The appropriate steam conditions are achieved through control of the boiler outlet conditions and the feedwater system.

Boiler outlet conditions
Steam turbines extract thermal energy from pressurized steam and convert it into rotational energy. The conversion is time-invariant; a fixed relation translates the input into the output. In this sense, the boiler outlet conditions can be interpreted as a transfer function between power demand and production. Therefore, the power output of a steam turbine is determined by the steam properties (pressure, temperature and flow) at the boiler outlet (i.e. turbine inlet) and the pressure in the condenser (i.e. turbine outlet). To obtain the desired power output it is essential to produce steam with the appropriate conditions.

In conventional power plants, the steam pressure is controlled by the Coordinated Control (CC)-system. The exact description and the implementation of this system is given in [8]. The CC-system is a master-slave configuration consisting of three modules (Figure 1-3): the Pressure Setpoint Calculation (PSC) module (master), the Boiler Pressure controller (slave) and the Turbine controller (slave). The CC-system is the main control system of any power plant and its objective is to achieve the desired power output ($Charge_{ref}$) [9, 8].

To achieve the desired power output, the PSC module uses the actual power output ($Charge$) and $Charge_{ref}$ to define fresh steam reference Pvv_{ref} (i.e. boiler outlet pressure). Pvv_{ref} is the desired pressure in the boiler and the turbine (i.e. pressure balance). Pvv_{ref} behaves proportional to $Charge_{ref}$. Therefore, for instance during power surplus (i.e. $Charge > Charge_{ref}$) also Pvv_{ref} is decreased. This initiates action in both the turbine and boiler controller. Hence, the PSC module coordinates the actions of both the turbine and boiler through Pvv_{ref}. The maximum value of Pvv_{ref} is given by $Pvv_{100\%}$, which represents the maximum allowable pressure in the boiler (constant value $136bar$).

The Turbine controller (feed-forward) uses Pvv_{ref} and Pvv to determine the steam requirement of the turbine, which is expressed in turbine (governor) valve position (Y_{hp}). By actuation of the turbine (governor) valve a certain mass flow steam, with pressure Pvv ($=Pvv_{ref}$ ideally), enters the turbine. As a result the turbine produces the required amount of power.

At the same time the Boiler Pressure controller (PC1, PID) uses Pvv_{ref} and Pvv to determine the required amount of heat (Q_{tot}) to maintain the pressure balance. In other words, how much fuel does the boiler need to produce the required amount of (fresh) steam. For example, when Pvv_{ref} increases more steam is required. To achieve this, the boiler is provided with more fuel (Q_{tot} increases) and consequentially the evaporation rate increases (more steam is produced). Note that this does not directly relate to an increased Pvv (evaporation = isobar). However, during the increasing evaporation rate the water level ($Nbal$) in the drum decreases. At the same time it is desired to maintain a constant $Nbal$, amongst others: to prepare for a next change in $Charge_{ref}$. Therefore, the feedwater system increases the water flow and this results in the desired Pvv ($= Pvv_{ref}$).

As changes in the $Charge_{ref}$ lead to differences in the heat production of the boiler, the temperature inside the boiler is also influenced. To keep the temperature around its specified reference (Tsh_{ref}), temperature control (TC1, PID) is required. This system regulates the temperature at the boiler outlet (Tsh) by water injection (I_{inj}).

In the process and instrumentation diagram (Figure 1-2) is shown how the control of the boiler outlet conditions is implemented in power plants.

Feedwater system

The feedwater system is responsible for the operating conditions in the boiler and the drum specifically. Reducing the oscillations in the feedwater system relates to many process aspects (e.g. temperature control and steam supply) but most importantly the operation of the evaporator [7]. The feedwater control system (PID - LC 1 and PC 2) controls the water level ($Nbal$) and the feedwater pressure by actuation of the feed pump speed (v_{pump}) and boiler valve position (I_{valve}) (Figure 1-2). The feedwater pressure is defined as the pressure difference between the feed pump and the drum (dP).

Taken together, the following process variables are considered in boiler outlet condition and feedwater control (Figure 1-3):

Pvv	The steam pressure at the boiler outlet (PC1 - A).
Tsh	The steam temperature at the boiler outlet (TC1 - B).
$Nbal$	The level in the drum (LC1 - C).
dP	The feedwater pressure (PC2 - D).

Please note that, the CC-system achieves the appropriate $Charge$ through the combination of boiler outlet condition, turbine and feedwater control. Therefore, $Charge$ itself is not considered as a part of boiler outlet condition and feedwater control. Also note that the control systems, discussed in this section, are in practice more complex than explained here (e.g. the steam temperature is in fact a PID based master-slave structure). Please refer to [8] for a full discussion of considered control systems.

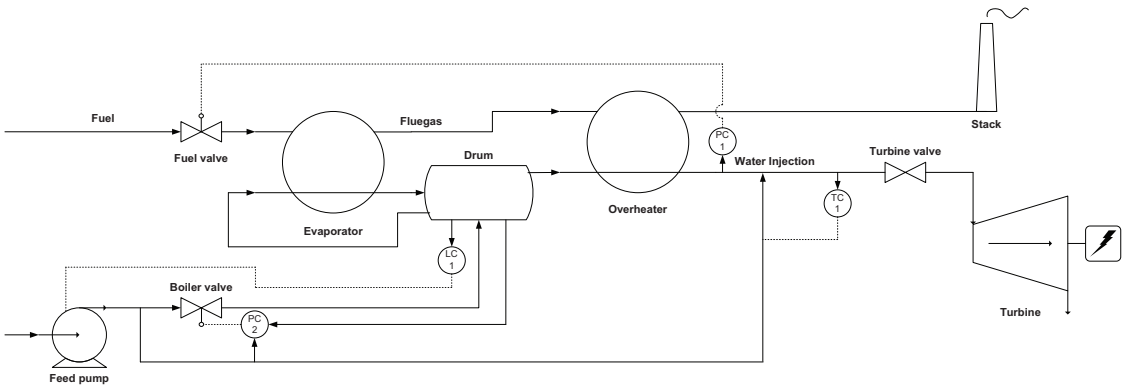

Figure 1-2: Process and instrumentation diagram: Boiler conditions & Feedwater system

The implementation of boiler outlet condition and feedwater system control is shown in Figures 1-2 and 1-3. Each control system bases its control action (Q_{tot}, I_{inj}, v_{pump} or I_{valve}) on the difference between the desired output, specified by references (Pvv_{ref}, Tsh_{ref}, $Nbal_{ref}$, dP_{ref}), and the actual output. All references are constant values (resp. $525°C$, $0cm$ and $31bar$), except Pvv_{ref} which is a trajectory. This trajectory is calculated by the Pressure Setpoint Calculation module and is based on the power demand, the current steam pressure and the maximum boiler pressure.

Note that Figures 2-3, 2-5, 3-7 and 4-2 show dP_{ref} around 0, this is a notation-choice. Since, the main focus is having a constant dP, its value of $31bar$ could make figures unclear. Therefore, the designer of the simulator opted to display: $dP\ -31bar$.

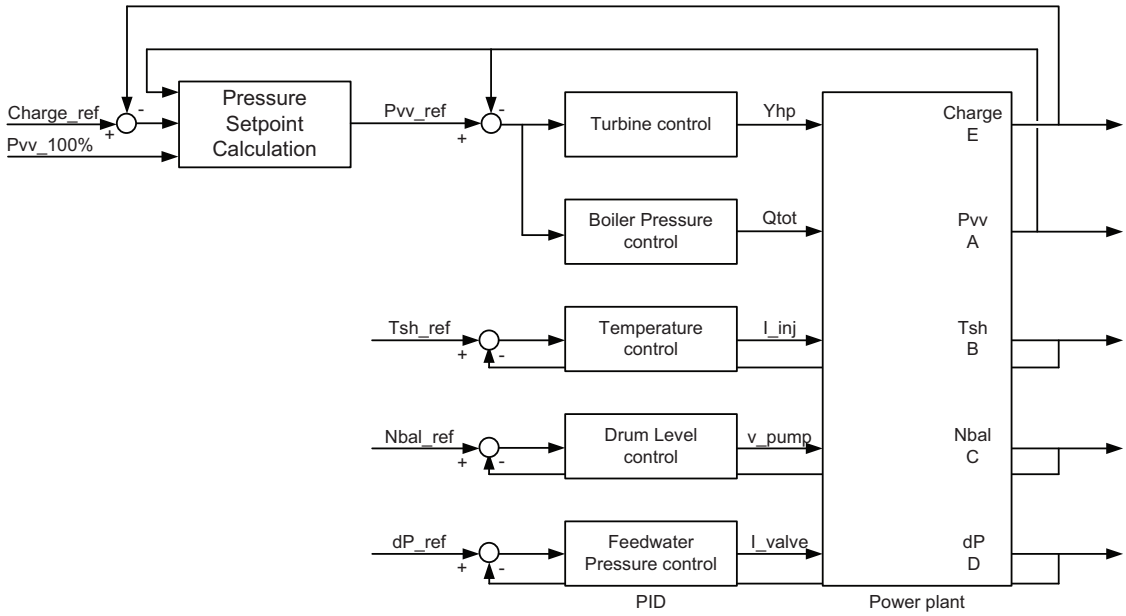

Figure 1-3: Control diagram: CC-control, Temperature control & Feedwater control

Previous research indicates that MIMO APC could improve the control of boiler outlet conditions (Pvv, Tsh) and the feedwater system ($Nbal$, Pvv) significantly. When successfully applied, MIMO APC could achieve smaller oscillations and settling time for both systems [2, 7]. Improved control of boiler outlet conditions is expected to translate directly to the output of the power plant, improving the overall performance and the efficiency of the power plant [10, 2]. While improvement of feedwater control contributes to achieving the desired steam properties.

1-3 Problem Statement

Summarizing the previous sections, the essence of the considered control problem is:
The negative influence of interaction effects, in the boiler outlet conditions and the feedwater system, on overall power plant performance during a change of power production.

These effects include the cross-coupling of different input/output variables and low control performance. Furthermore there is considerable oscillation in the specified controlled variables (Pvv, Tsh, $Nbal$ and dP) as well as the other plant variables. APC provides the possibility to achieve both decoupling and a better performance.

To adress the defined control problem, the following problem statement is considered:

Considering a power plant and a realistic power demand signal, design a MIMO advanced process controller that reduces oscillation and increases the performance of process variables.

The problem statement leads to the following two research questions:
- To which extent can MIMO APC reduce the oscillations in the process variables?
- To which extent can MIMO APC increase the performance of the process variable control loops?

Elaborating on the problem statement the following clarifications are made:
- The considered power plant is PID-controlled. The influence of MIMO APC is evaluated through comparing process variable behavior in the initial power plant and the power plant modified with MIMO APC.
- The realistic power demand is defined as a scenario (Section 2-2).
- The considered process variables are: the steam pressure and temperature at the boiler outlet, the drum level and the feedwater pressure.
- Reduction of process variable oscillation is considered significant when the amplitude decreases with at least 5% [2].
- Control performance is evaluated through settling time, rise time and steady-state offset of the controlled process variables. A performance increase is considered significant when one or more evaluation values are reduced with at least 5%.

Decoupling is evaluated through the oscillation amplitude (term definition, see: B-3) of the controlled variables. Finally, a boundary condition of the control design is that it is robust (as defined in [4]). We considered a controller robust when it fulfills the basic robustness criteria (Chapter 3).

1-4 Approach

In this section, the research strategy is outlined. The main concepts and choices of the research are presented and motivated.

Summarizing the problem statement, this investigation aims to design an APC which reduces oscillations and increases the performance for a set of process variables during a change in $Charge_{ref}$. Achieved results are evaluated through comparison to initial, PID controlled, power plant behavior. Comparing the two (i.e. PID to APC) will indicate the room for improvement, achievable through APC.

For this aim, Laborelec has provided a power plant simulator (Simulink). The simulator is considered equivalent to a conventional thermal power plant. Since the simulator is not validated, this investigation will mainly focus on the design and testing of a new control concept rather than building a controller for direct implementation. In practice this does not change the execution of the investigation. However, the results of this study should be interpreted with care.

Instead of using the original simulator (Sim_{orig}), this investigation will be done on a modified simulator (Sim) which represents a gas- or oil-fired conventional power plant. The modifications align the simulator to the problem statement, especially the aspect of estimating the performance improvement capacity of APC.

Making use of Sim, next step is to derive a linear model. The obtained model is a key component for the investigation, as it is a prerequisite for the used controller synthesis-algorithm. Hereafter, the actual control design (selection of weighting method and the synthesis) and tuning takes place. All found controllers are applied to the linear model. Here, the linear model is considered the nominal plant. The controller that performs best, with respect to reduced oscillation and increased performance, is selected. The selected controller is applied to Sim. Sim is considered as nominal plant with uncertainty. To measure the effects of APC, a simulator with and without APC run the same scenario (defined experiment). For evaluation, both results are compared and the difference in oscillation and performance is quantified. The results will lead to a set of conclusions on the research questions and a corresponding discussion. Finally some future directions are outlined.

To derive the linear model and to implement the APC into the simulator a certain infrastructure is required: the control structure. Basically the control structure defines what the inputs and outputs of the linear model and simulator with respect to the controller are. Based on this definition the linear model is derived and the simulator is modified. There are two common ways to implement APC:

- Replacing the current control system with the APC.
- Use APC on top of the current control system.

Previous research indicates that it is, due to its stabilizing influence, not favorable to replace the current control system [7]. This is also motivated by the practical objections, as discussed in the introduction. Therefore MIMO APC will be used to complement the current PID-control system. The PID-system will not be modified given its role in stabilizing the power plant and its addition to safe power plant operation. Moreover, the PID-system serves as a back-up system in case the APC fails. Furthermore, adding APC to a functional control system is more cost-effective than replacing the entire plant control system.

For APC of large scale industrial processes, like power plants, two control methods are commonly considered: Model Predicitve Control (MPC) and H_∞-control. In industrial practice MPC is commonly preferred, since it (amongst others) is possible to define the desired process conditions explicitly. However, in this investigation is it chosen to use H_∞-control. Three main arguments motivate this choice [4]:

1. H_∞-control is able to cope with unstable plants (required for operation of the drum).
2. H_∞-control is able to cope with uncertainty (which is expected to occur for the simulator). Since MPC is not designed to consider uncertainty it is very weak in this area.
3. H_∞-control is implementable through a set of fixed transfer functions, while MPC requires model based real-time optimization.

The influence of the selected control method is not considered further in this research. To combine selected control method with the desired control structure the following master-slave structure (Figure 1-4) is proposed.

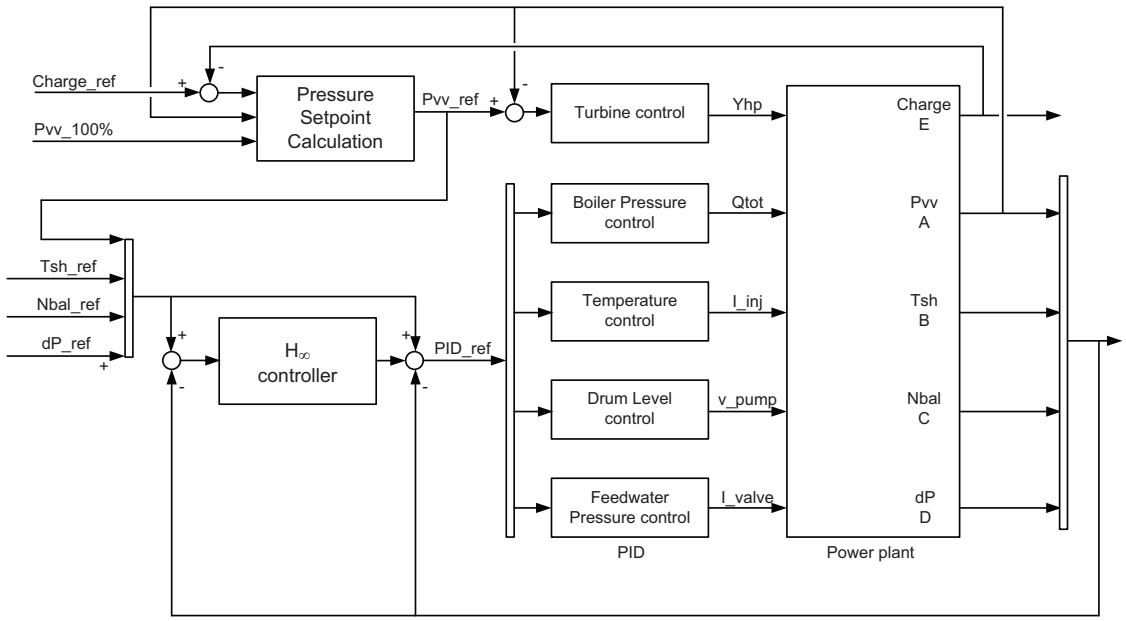

Figure 1-4: Control diagram: proposed H_∞-control-structure

Figure 1-4 shows the aimed physical implementation of the controller in the simulator. Since it is quite a complex presentation, Figure 1-5 shows the control structure schematically. The conventional controlled power plant is presented by the closed-loop combination of controller K and plant G. In this combination, K uses error signal e (difference between reference y_{ref} and actual output y) to generate control signals u. Control signals u are fed into plant G and aim to produce the desired output ($y = y_{ref}$). Now expanding the conventional system with APC, references include instructions to compensate for multivariable effects. The required compensation instructions are calculated through considering again $y_{ref} - y$. The instructions are fed to the conventional system as a set of small corrections (i.e. small changes) in the reference values (Δy_{ref}).

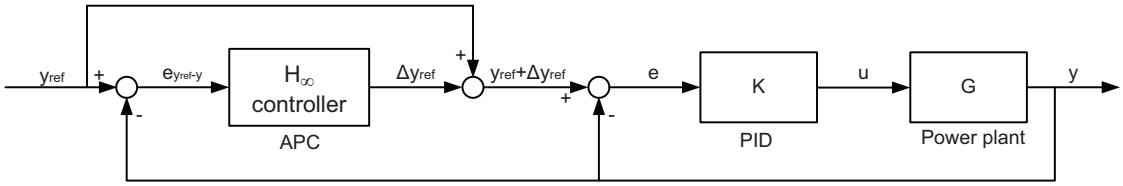

Figure 1-5: Schematic: proposed H_∞-control-structure

The conventional (PID) system now serves as a slave receiving compensated reference signals from the H_∞-controller (master). However from perspective of the PID, the small differences in reference are not a big change (only that y_{ref} is not fixed anymore). Hence, it is possible to implement this multivariable system, almost without changing the conventional system. The combination of PID- and H_∞-control, considers and deals with coupling and disturbances [4]. However, in case of an emergency, it is possible to shutdown the H_∞-controller almost without disturbing normal operation of the PID system.

There are several methods available to design weights for H_∞-control-synthesis (e.g. S/T, $S/T/K$ and S/KS). Each method is equipped to address a specific problem type, for instance the S/T method is well suited to improve tracking and the S/KS approach is well suited for synthesis of disturbance rejection H_∞-controllers [4]. Based on the problem description weights should produce a controller that achieves decoupling, which ideally prevents that changes in $Charge_{ref}$ (which directly translate to Pvv_{ref}) cause oscillations in the other process loops (Tsh, $Nbal$, and dP). This is achievable with each of the three weight synthesis method by selecting diagonal weights (all off-diagonal terms are zero, i.e. requiring decoupling). In practice, it is often not possible to completely eliminate coupling this way. Furthermore, also throughput changes will continue to influence all process loops. Therefore, some (reduced) oscillations will continue to occur. From perspective of process loops (e.g. Tsh, $Nbal$, and dP), the influence of throughput changes are disturbances (causing oscillation). Hence, to reduce the effects of the disturbance it is desired to desing a controller that can achieve more effective disturbance rejection. Therefore, the S/KS method is selected for weight design. Please note, sensitivity function: $S = (I + GK)^{-1}$ and control sensitivity: KS.

Summarizing the approach, the objective of the to-be-designed control system is to keep the process variables (Pvv, Tsh, $Nbal$, dP) around their specified references (see Section 1-2) during and after changes of $Charge_{ref}$. Also note that this approach is designed to show the possibility to improve control of a set of internal control loops (loops: Pvv, Tsh, $Nbal$, dP) for a given power plant while observing the effects this has on its overall behavior (i.e. the $Charge$-loop). It should be clear that improved internal control is only acceptable when overall power plant behavior improves (or at least not decreases).

1-5 Report Structure

This section presents an overview of the structure of this report. The structure is based on the presented research strategy (Section 1-4), objective is to research the defined hypotheses (Section 1-3).

As discussed in the approach (Section 1-4), a linear model is required. This model will be derived from a simulator using system identification (Section 2-4). The model linear will serve as a base for control design (Section 3-3). The tuning of the controller is based on the performance it achieves on the linear model. If the controller performs well and if further tuning iterations have little improving effect, the controller is selected for application to the simulator (Section 3-4). If necessary, redesign is done. This results in the final controller and its performance (i.e. performance of the simulator with the final controller) is evaluated (i.e. compared to the initial simulator). Based on the results the research questions are answered (Chapter 5) and an answer to the defined problem statement is found. Furthermore, the results will be the base for a set of conclusions and a discussion with a few reccomendations.

This leads to the following report structure:
- Chapter 2: Simulator Modifications and linearization.
- Chapter 3: Improving Performance with Advanced Process Control.
- Chapter 4: Improving Flexibility with Advanced Process Control.
- Chapter 5: Conclusions, Discussion and Future Directions.

Chapter 2

Simulator Modifications and Linearization

To investigate the defined problem statement, Laborelec has provided a power plant simulator. The simulator is considered equivalent to a real power plant. Hence, all experiment and design work is based on or aimed at application to the simulator. During this study, the simulator is used for two main purposes, namely: the derivation of a linear model (Section 2-4) and the evaluation of the designed controller (Section 3-4). This chapter focuses on the derivation of the linear model, starting with a brief description of the simulator (Sim_{orig}). After this, to evalute the behavior of the simulator, a scenario is introduced. For comparison, this scenario is used throughout the entire study. The behavior of the simulator is evaluated and as the simulator was not designed for the purpose of this investigation a set of modifications are proposed. The modifications are implemented using the programmed adaptability features in the simulator and redefine the simulator as a gas-fired drum-boiler power plant. Hereafter, the effects of the modifications are measured and evaluated. Finally, the modified simulator (Sim) is used to derive a linear model (Mod).

2-1 Power Plant Simulator

In 2006 Laborelec, the research institute of Electrabel, has developed a power plant simulator. The result is a user-friendly simulator that provides insight in the physical processes in power plants. Furthermore, the simulator design is easily adaptable to simulate other power plants. The simulator provides the possibility to design and test new control concepts without the costs and safety issues of real-life experiments.

Figure 2-1: Les Awirs power plant

The simulator [8, 11] is an idealized yet complex model of Les Awirs 4 (Figure 2-1) which was, when the simulator was build, a real $135MW$ coal-fired drum-boiler power plant unit located in Liege, Belgium. In the simulator all power plant components (e.g. the boiler, turbine and condenser) are modeled. The model includes the thermodynamic, fluids and mechanical properties of the process. Next to this also the control system is modeled. The simulator is written in Simulink and it can easily be used in combination with Matlab.

2-2 Scenario

As for real power plants, operation of the simulator is based on the power demand ($Charge_{ref}$). Although many external factors contribute to and determine the power demand, individual power plants only see $Charge_{ref}$. Hence, to run a simulation only a scenario describing $Charge_{ref}$ is required. After this, simulation is done and data is produced which shows the behavior of the power plant (simulator). Making use of this fact, it is possible to simulate all kinds of events.

In this study, the used scenario only facilitates the design and evaluation of controllers. Motivated by the aim to obtain insight in the potential of MIMO APC for real power plants, the scenario is inspired on process conditions during real-life events. Furthermore, it respects the constraints and limitations of the simulator. The use of a scenario also ensures equal comparison during experiments that are done twice, e.g. comparison of the original and modified simulator. The following scenario is introduced:

$Charge_{ref}$-change scenario
The $Charge_{ref}$-change scenario simulates a $35MW$ ramp in the power demand (from $135MW$ to $100MW$) with a gradient of: $5MW/min$. This is a substantial decrease in the power demand, moreover the magnitude of this decrease requires the Pressure Setpoint Calculation module to use both the Turbine and Boiler Pressure controller. This event introduces large oscillations in the considered process loops. Therefore, it is reasoned that this scenario tests the power plant control systems under extreme conditions. This scenario is used to evaluate the problem statement by comparison of the original, PID controlled, simulator and the new H_∞-controlled simulator.

Note that it takes about 7 minutes before $Charge_{ref}$ reaches its final value. Furthermore, the power plant requires up to $4000s$ to reach steady-state. Hence, the length of this scenario is at least $8000s$ ($4000s$ to reach steady state after starting the simulator, and another $4000s$ to do the experiment).

2-3 Simulator Modification

In accordance with the approach the simulator will be modified. Aim of this section is to present a detailed description of the modifications (Section 2-3-2) and their effects (Section 2-3-3). Furthermore, will be discussed why these modifications are allowed. The provided simulator will serve as a starting point and before doing modifications its behavior will be evaluated (Section 2-3-1).

2-3-1 Introduction

To investigate the normal behavior of the provided simulator an initial experiment is done. In this experiment, the $Charge_{ref}$-change scenario is runned on the simulator (Sim_{orig}) while the 4 specified outputs (Pvv, Tsh, $Nbal$ and dP) are measured. The resulting behavior is shown in Figures 2-2 and 2-3.

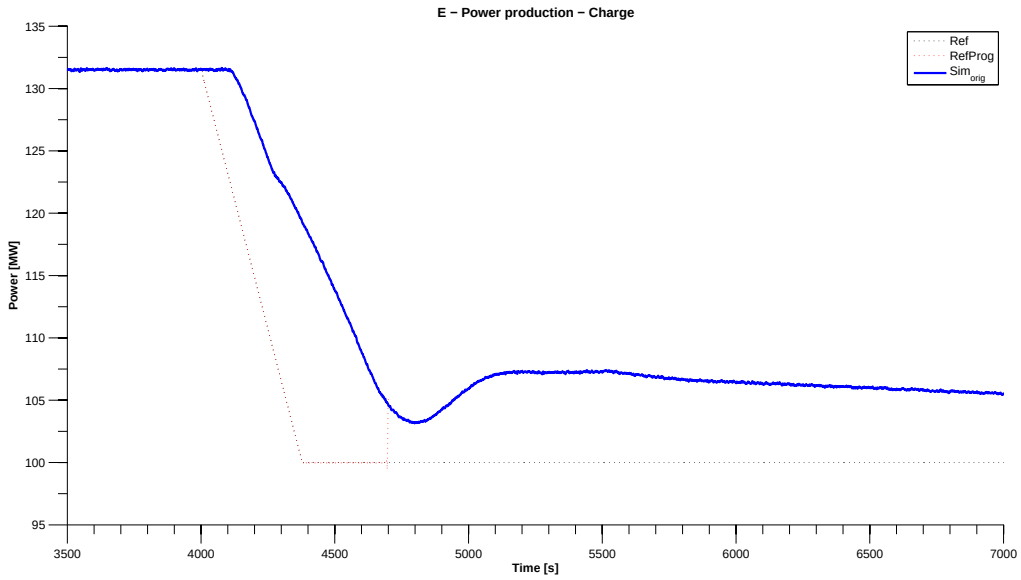

Figure 2-2: Original simulator (Sim_{orig}) response: $Charge$

From Figure 2-2 we observe that the $Charge$-signal does not reach its defined $Charge_{ref}$. However, the $Charge$-signal does follow defined $RefProg$-signal (the $RefProg$-signal represents how the PSC-module interprets the defined reference). This behavior is not expected and is adressed further below.

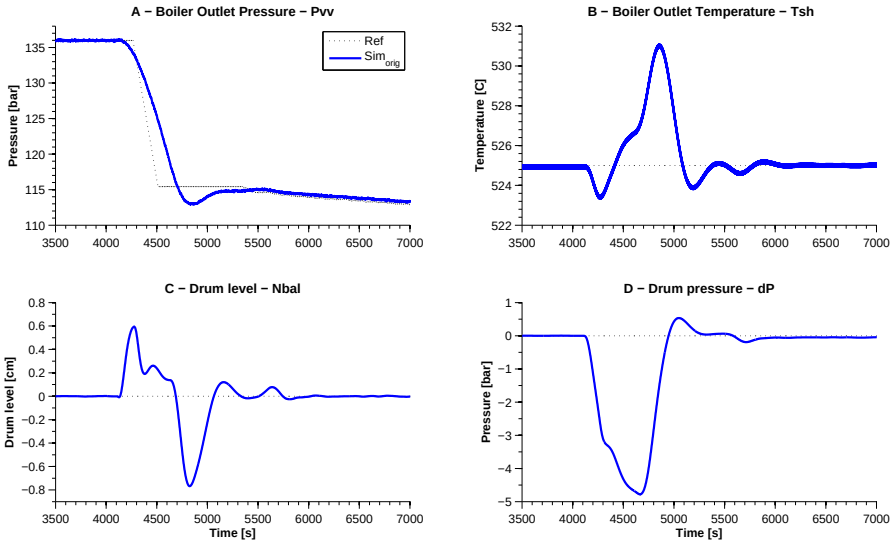

Figure 2-3: Sim_{orig} response: Plant outputs

From Figure 2-3 is observed that the simulator has reached steady-state at the start of the experiment ($4000s$) and the defined references (Pvv_{ref}, Tsh_{ref}, $Nbal_{ref}$, dP_{ref}, Section 1-2) are respected. Process variables Pvv, Tsh, $Nbal$ and dP display the expected oscillations, that occur under influence of the $Charge_{ref}$-change scenario. After a while the oscillations are successfully rejected and the process returns to its references in a limited amount of time. Hence, considering the response of Pvv, Tsh, $Nbal$ and dP it seems that the simulator operates as expected.

In Section 2-1 is mentioned that the simulator describes formerly coal-fired power plant Les Awirs 4. In coal-fired power plants, pulverized coal is used for fuel. To produce the pulverized coal, power plants are equipped with very large coal mills. In these mills, coal is grinded until the desired particle size is achieved. However due to high flammability and corresponding safety risks, coal milling only happens on-demand. This introduces a substantial dead-time in the fuel flow, which means that a change in power demand is also fulfilled with a large dead-time (Figure 2-2). The large process dead time will importantly limit the control [12] and overall plant performance.

As can be seen in Figure 2-2, the power output ($Charge$) response settles with an offset (about $5MW$). However, in Figure 2-3, the steam pressure (Pvv) nicely follows its reference which is defined by the PSC-module. Apparently, there is a problem in the PSC-module which causes Pvv_{ref} to be too large. Furthermore, Pvv_{ref} does not converge to the pressure that is required to reach $Charge = 100MW$. Study of the Pressure Setpoint Calculation module revealed that this is caused by the tuning of the Pressure Reference Correction controller (PRC). The PRC-controller is a part of the PSC-module (see next section for further details on the PRC). Although this behavior is present in the provided simulator and while it does not leads to abnormal results or critical simulator failures, it is undesired and we will solve this problem by retuning the Pressure Reference Correction controller.

2-3-2 Methods

Considering the problem statement, it is undesirable to research the potential of APC while its achievable performance is substantially limited by the properties of the power plant (expressed by the simulator). Therefore, it is proposed to change the behavior of the simulator fuelling system into that of a gas- or oil-fired conventional power plant. In these power plants the fuel flow dead-time is very small (about $3s$), which allows its influence on control performance to be neglected.

Reduce boiler dead-time
For practical reasons the simulator does not include a complete boiler model. Instead a simplified boiler is modeled with 10 transfer functions. These transfer functions reproduce the response of a coal-fired boiler, including the fuel system dead time (80 to 120s). Thanks to the flexible simulator design, the fuel system dead time can be reduced (to 3s) by the change of only 2 constant values (Temps mort du broyeurs [boiler] and Guestion des modes du GR [turbine controller]). It is reasoned that the behavior of the simulator now describes Les Awirs 4 would it have been using gas or oil for fuel.

Retune boiler controllers
Without the dead time, the fresh steam production has become faster. Hence, to utilize this also the Boiler Pressure Controller should be retuned (faster). Retuning is done based on the IMC tuning rules [13], tuning objective is: achieve a low settling time while having no (or very limitted) overshoot.

To reduce the observed offset, the PSC-module has been analyzed. Analysis showed that the PSC-module calculates the pressure reference using a ramp generator (GR) and a Pressure Reference Correction (PRC) controller. It seems that during small changes in $Charge_{ref}$, the reference Pvv_{ref} is calculated by the GR alone (the PRC does not seem to work at all). For large changes ($\pm 35MW$) also PRC is active (but it does not work correctly). During these large changes, for instance the $Charge_{ref}$-change scenario, GR ramps Pvv_{ref} down to about 10bar above the actual required pressure reference. When Pvv reaches the defined pressure, the PRC is activated and it should calculate a smooth trajectory for the last 10bar. The objective of this layered structure is to stably decrease the pressure as fast as possible. However, it does not seem to work correctly in Sim_{orig} and as a result the offset occurs.

Analysis of the PRC reveals that it is caused by its tuning (large settling time, about 1000s, and large steady-state offset). Furthermore, it is set to wait too long after Pvv has reached Pvv_{ref} (about 660s). Therefore, the PRC should be retuned.

Replacement of Xsteam
The external Matlab function Xsteam calculates the thermodynamic properties of water for many of the processes in the simulator. Based on two input signals (example: pressure and enthalpy) Xsteam looks up the desired property (example: temperature). Xsteam is a very complex program with multiple functions. In the simulator only a few of the basic functions of Xsteam are used and although largely unused the entire program is evaluated. This is considered unnecessary complex. Therefore a set of basic look-up tables will be used instead. The data for the lookup table is generated by running Xsteam for certain data sets.

2-3-3 Results

The dead time has been reduced according to plan and also Xsteam has been replaced. Furthermore the IMC retuning procedure resulted in different PID controller settings (compared in Table 2-1).

	K_c	τ_i	τ_d	τ_f
Initial	4	315	0	1
New	4	267	0	1

Table 2-1: PID-controller tuning: old & new settings

Furthermore, choosing the PRC controller twice as fast as the Boiler Pressure controller results in a fast and smooth response when activated. For the waiting time a much lower value is selected (to $1s$).

These modifications change the simulator behavior. To visualize and asses this change, the modified simulator (Sim) is compared to the original simulator (Sim_{orig}). Again the $Charge_{ref}$-change scenario is applied, resulting in Figures 2-4 and 2-5.

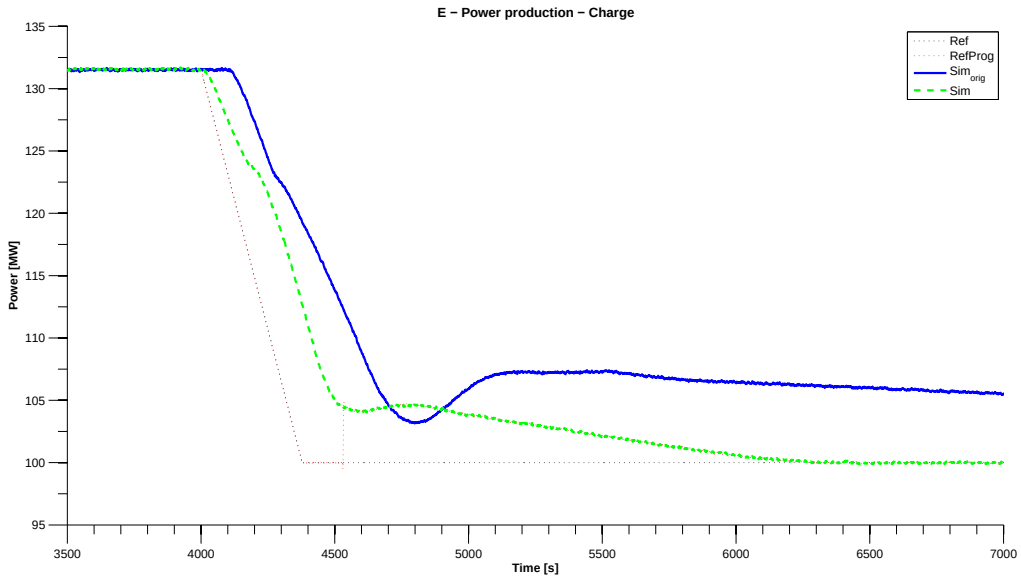

Figure 2-4: Responses of Sim_{orig} and Sim: Charge

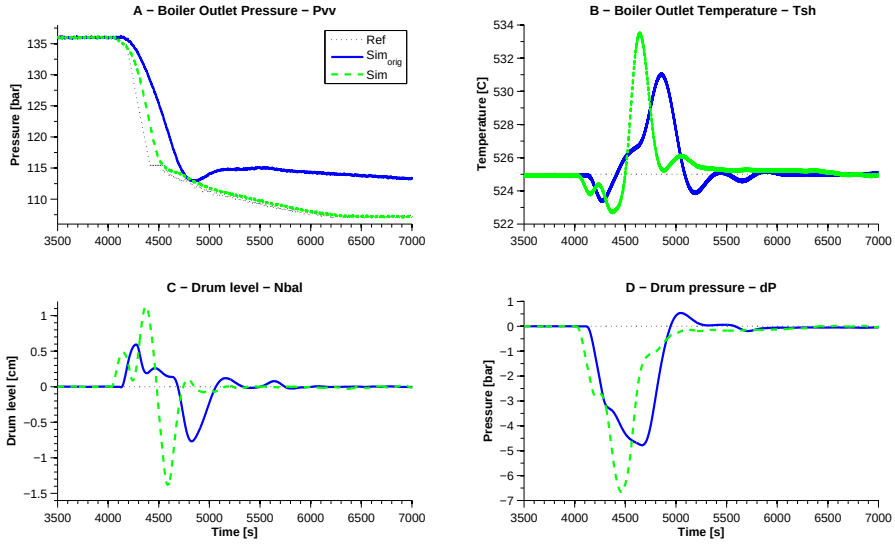

Figure 2-5: Responses of Sim_{orig} and Sim: Plant outputs

In Figures 2-4 and 2-5, the modified simulator (Sim) is compared to the initial simulator. It is observed that both simulators reach steady-state before $4000s$ and each process variable (Pvv, Tsh, $Nbal$ and dP) has reached its reference value. During the $Charge_{ref}$-change scenario all process variables are excited. After a while all process variables return to their reference.

Comparing the two simulators, the modified simulator shows the following three differences:

1. Every variable ($Charge$, Pvv, Tsh, $Nbal$ and dP) reacts at exactly $4000s$.
2. Each variable follows its reference.
3. The peaks of the variables are higher.
4. The variables settle faster (lower settling time: about $120s$).

Based on these observations is concluded that the dead-time has successfully been reduced and that the issue with the PRC is solved. The behavior of Sim is still roughly equal to that of Sim_{orig}. Due to the reduced dead-time, the stability and performance margins of Sim have increased slightly resulting in better simulator performance. Furthermore, the faster boiler is reflected in the shape of the process variable oscillations (they also have higher peaks). Sim corresponds to the defined problem description, hence this simulator will be used for linearization.

From practical point of view Sim has two major advantages, namely due to the replacement of Xsteam the calculation time has decreased 5 times and the offset is resolved.

2-4 Linear Model

In this section a linear model (Mod) is derived from the modified simulator (Section 2-3). To obtain the linear (state space) representation two methods are available. Each method will be described in Section 2-4-2. Both methods are applied and as a result a linear model is obtained (Section 2-4-3).

2-4-1 Introduction

In this section a linear model is derived, this is motivated by the following two arguments. Synthesis of H_∞-controller requires the linear representation of a the to-be-controlled system [14]. Furthermore, due to calculation time it is unpractical to use the modified simulator for the actual control design.

For control of the boiler outlet conditions and the feedwater system the linear model will have the following 4 inputs:
- Boiler pressure loop (Pvv_{ref}).
- Boiler temperature loop (Tsh_{ref}).
- Drum level loop ($Nbal_{ref}$).
- Feedwater pressure loop (dP_{ref}).

And the simulator response for these loops (Pvv, Tsh, $Nbal$ and dP) are the 4 outputs.

2-4-2 Methods

Considering the available Simulink model, two methods are available to derive the linear model, namely: linearization and system identification.

Linearization
Simulink provides the possibility to directly linearize the modified simulator using LINMOD, a standard linearization tool in Matlab. LINMOD is a very basic tool that only requires the specification of the to-be linearized inputs and outputs. Also an operating point should be specified. When this is done, the algorithm automatically produces a linear model [15].

Although LINMOD is not usable in industrial practice (an actual plant), there are several arguments motivating its use in this study. In previous research, good results have been obtained using LINMOD [7]. Furthermore, when a Simulink model is available, LINMOD is a very simple and effective tool to derive linear models. For the successful derivation of linear models using LINMOD, significantly less knowledge of the to-be-linearized model is required and it is also very time effective. Considering these arguments, it is clear that LINMOD is the preferred method to derive linear models.

System identification

System identification is a method to determine the behavior of a system by exciting its inputs and observing the resulting output responses. For successful application of system identification extensive knowledge on the to-be-identified system (e.g. physical limitations, stability margins, noise presence) is required, also the procedure complexity is high (e.g. safety, identification costs, time, accuracy and identification signal design). However, system identification is the only possible method to derive models in industrial practice (an actual plant). Furthermore, internal (simulator) modeling does not influence the identification procedure. This is an important advantage when using a very complex simulator. Therefore, system identification will be used next to linearization. Additional advantage is that, in case both methods are successful, two independent linear models are available for comparison.

The identification procedure starts with a steady-state simulator, working at the desired operating point. The considered loops: Pvv, Tsh, $Nbal$ and dP are at their steady state values (resp. $136bar$, $525°C$, $0cm$ and $30bar$). The identification data is produced in 4 experiments. During each experiment one input is excited and measured while the others remain at their steady-state value (these are not measured). Furthermore, all 4 output signals are measured.

To illustrate the identification procedure, look at the steps taken to identify the Pvv-loop. First the simulator is brought to steady-state (Pvv=Pvv_{ref}= $136bar$). Then at a certain time, Pvv is excited through application of excitation signal ΔP (Pvv_{ref}+ΔP). This produces a response at all considered outputs: Pvv, Tsh, $Nbal$ and dP. During this experiment 1 input and 4 output signals are measured (1 excited input signal and their 4 output signals).

This procedure is repeated for each input separately until each input is excited once. Table 2-2 clarifies the setup of each identification experiment.

Exp	Excited input	Constant inputs (not measured!)	Measured Outputs
1	Pvv_{ref}	Tsh_{ref}, $Nbal_{ref}$, dP_{ref}	Pvv, Tsh, $Nbal$, dP
2	Tsh_{ref}	Pvv_{ref}, $Nbal_{ref}$, dP_{ref}	all 4
3	$Nbal_{ref}$	Pvv_{ref}, Tsh_{ref}, dP_{ref}	all 4
4	dP_{ref}	Pvv_{ref}, Tsh_{ref}, $Nbal_{ref}$	all 4

Table 2-2: Amplitudes of the identification signals

As previously discussed, excitation of plant inputs result in a certain response at the plant output. The properties (e.g. magnitude and shape) of the measured output response depend mainly on the properties of to-be-identified plant (i.e. system dynamics) and the excitation signal. Hence, for successful identification the design of the excitation signal is essential. Design choices include amongst others specification of shape, amplitude, frequency content and power distribution.

However, in this study has been opted for a more practical approach. During normal daily operation the "oscillations under investigation" occur when $Charge_{ref}$ changes. $Charge_{ref}$ is used by the PSC to calculate a new Pvv_{ref} (ramp signal). Through coupling, the change of Pvv_{ref} is reflected in not only Pvv but also in the other outputs and this is the exact phenomenon that is under investigation. Hence, this motivates the use of a similar ramp signal for excitation. However, it is hypothesized that the same effect is obtained with a step shaped excitation signal. Furthermore, it is reasoned that a step shape achieves more excitation and is more convenient in the identification procedure (finding the relation between in- and output and validating the behavior of a found model). Based on these arguments is chosen to use a step shape signal for identification.

Preliminary experiments with the simulator showed that it takes about $3000s$ to reach steady state. Therefore, including some extra margin, the excitation signals will be $4000s$ long (step time = $4000s$). Initially, the oscillation amplitude (see Figure 2-5) in the process loops was used as step size (for Tsh: $8°C$; $Nbal$: $3cm$; dP: $7bar$ and for Pvv: $5bar$). However, experiments with these values did not produce the desired excitation. The oscillations in Tsh, $Nbal$ and dP were not comparable to those in Figure 2-5. Therefore, the step amplitudes have been tuned (in- and decreased) until this was the case. The following step amplitudes have been found (Table 2-3):

	Pvv_{ref}	Tsh_{ref}	$Nbal_{ref}$	dP_{ref}
Excitation	$+7bar$	$+10°C$	$+5cm$	$+5bar$

Table 2-3: Amplitudes of the identification signals

As expected from computer-based simulation and data acquisition, the power plant simulator operates in discrete time. The solver, behind the simulator normally operates with variable sampling time. To simplify the identification procedure, the simulator solver is changed to fixed-sampling time ($h = 0.5$). This also fixes the sampling time of the provided (to the simulator) identification signal. However, the in- and output signals are measured (i.e. recorded) in 7 separate tracks, each with a different sampling time (range: 0.5, 10, 20, 40 and 80). The range has been calculated using the rule of thumb as discussed in [16] and is based on the found upper and lower limits of the 4 loops. Since the considered process loops are a combination of very fast and very slow processes (resp. the DrumLvl and Pvv-loop) the whole range has been considered during preliminary identification experiments. Results revealed that a sampling time of $h = 10$ produces the best fits for all loops (highest fit percentage) and is therefore selected as sampling time.

All properties of the identification signal have been determined. However, to conduct the identification experiment also validation data is required. This data is used to check that the 16 found transfer functions are also an accurate representation of the simulator in a different situation. To produce validation data, the inverse excitation signal (same amplitude but opposite direction) is applied to the simulator (e.g. for the Pvv-loop: $Pvv_{ref} - \Delta P$).

In practice, we will produce the validation and identification data through a single experiment. The experiment is designed as follows: the simulator is started and is allowed to reach steady-state (time: from 0 to 4000s). Hereafter the step-down (validation data) takes place and the simulator is again allowed to reach steady state (from: 4000s to 8000s). Finally the step-up takes place (identification), which returns the simulator to its initial state, and the simulator is again allowed to reach steady-state (from: 8000s to 12000s).

The full validation-identification signal for the 4 inputs (Pvv_{ref}, Tsh_{ref}, $Nbal_{ref}$ and dP_{ref}) are shown in Figures 2-6 to 2-9. These figures also show the corresponding output responses of Pvv, Tsh, $Nbal$, dP and the identification-results (i.e. the responses of Mod for the provided inputs).

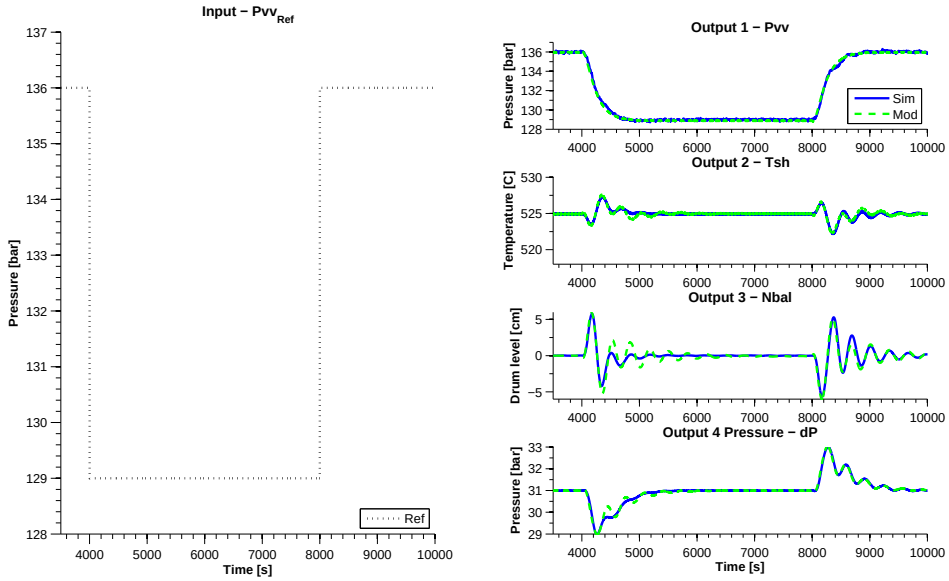

Figure 2-6: Identification experiment 1: Responses of Sim_{orig} and Sim

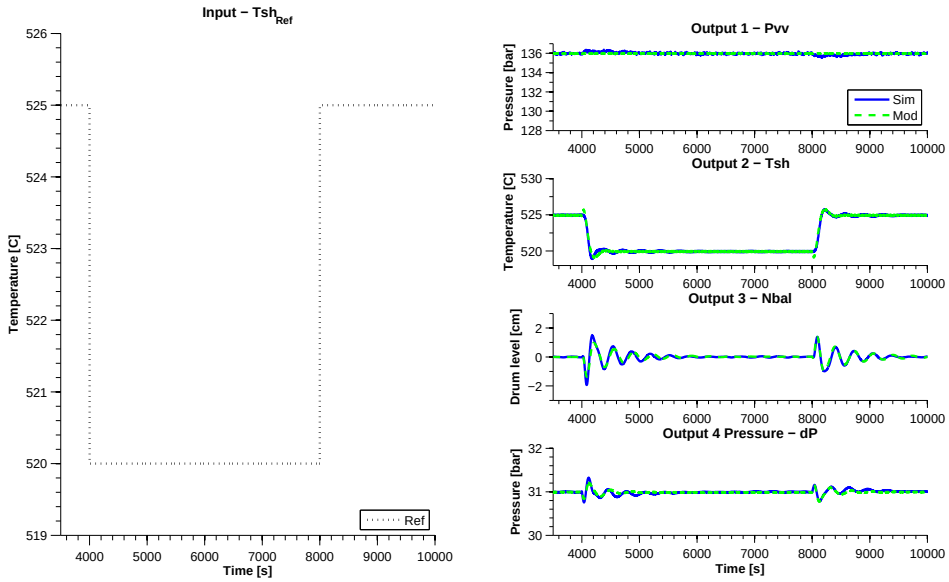

Figure 2-7: Identification experiment 2: Responses of Sim_{orig} and Sim

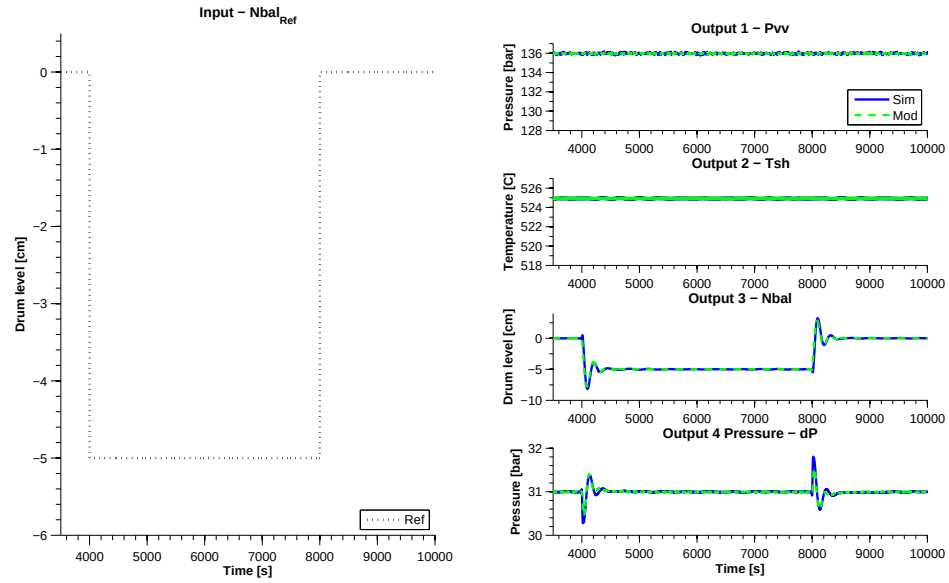

Figure 2-8: Identification experiment 3: Responses of Sim_{orig} and Sim

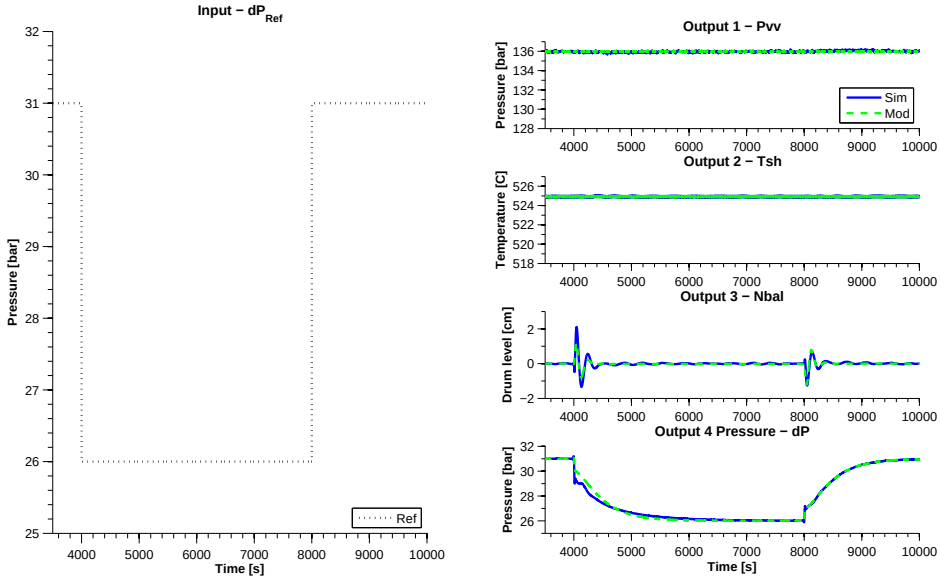

Figure 2-9: Identification experiment 4: Responses of Sim_{orig} and Sim

Four input signals and 16 (output) responses are obtained. The full validation-identification signal and their corresponding responses are not directly used for the actual identification. First, data pre-processing is done. The full signal is split in two parts: the validation part (by taking the signal from $4000s$ to $8000s$) and the identification part (from: $8000s$ to $12000s$). Furthermore, the responses and the identification signal consist of the absolute values (example: $Pvv_{ref}+\Delta P$), while the identification is done using deviation variables (example: ΔP). Therefore, the mean value (e.g. $136bar$ for Pvv_{ref}) is subtracted from the validation and identification signal. The identification and validation signal are now each $4000s$ long and only concern the excitation signal (e.g. $+$ or $-\Delta P$) with their response.

After pre-processing, the input signals, output data and the validation data is ready for use in identification. Linear models are identified by mathematically relating input signals to their (output) responses. The identification is done with the standard Matlab (2007b, version 7.5.0.342) system identification toolbox: IDENT (System Identification Toolbox 7.1).

For identification, it is required to load the identification- and validation-data into IDENT. Looking for instance at set 1, with excitation signal: Pvv_{ref} and output responses: Pvv, Tsh, $Nbal$ and dP, 8 sets of data are loaded into IDENT (for each combination, e.g. Pvv_{ref} to Pvv, both the identification and validation data). Next to this, for each set IDENT requires the specification of the signal data type (Time-Domain Signals), the name of the data set (e.g. $PrPvv1$ for the validation part and $PrPvv2$ for the identification part), its starting time ($0s$) and the sampling interval ($h = 10$). Hereafter, IDENT provides the possibility of pre-processing the data but this is already done.

The actual system identification starts with the selection of working data (e.g. $PrPvv2$), the validation data (e.g. $PrPvv1$) and the estimation type (linear parametric model). Before estimation, IDENT requires the selection of a desired model structure, model order, model name, estimation method and estimation preferences (focus, initial state, covariance). Since we are only looking for a representation of the system dynamics, the used model structure is Output Error (OE). However, to check whether OE was the best structure also other model structures (e.g. ARX and State-Space) have been tested for all (16) transfer functions. Note that in this procedure, each transfer function is identified separately.

Selection of model structure and model order is based on 3 points of evaluation, first and most important is the step response of the identified linear model. The main question: is the step response (to a high degree) similar to the measured response of the plant. This property is evaluated visually and it shows the behavior of the linear model independent on the identification data. The other 2 evaluation points are only considered, when the response of the linear model shows the same behavior as the plant. This is already a strict selection of possible model structures and model orders. Hereafter, is evaluated how well the linear model describes the validation data using a fit percentage. A higher fit percentage means that the linear model fits the validation data better (i.e. more accuracy). Finally is also evaluated how much the fit percentage improves when the model order is increased.

This procedure provides the possibility to trade-off complexity (i.e. model-order) to accuracy (i.e. fit percentage) per transfer function. We want to derive a linear model that has the lowest model order that provides good accuracy (i.e. increasing the model order further has a small influence on accuracy). The lowest possible model order is amongst others motivated by the fact that the to-be-derived H_∞-controller will be of the same order, which could cause numerical problems. Other arguments supporting this procedure are presented in [16].

Note that this identification procedure also allows inclusion of a priori knowledge of the power plant system. For example, the identification data obtained for loop dP_{ref} to Pvv resulted in a signal with a very low signal to noise ratio. This seems strange since dP_{ref} determines the feedwater pressure (hence ultimately also Pvv). However, with a priori knowledge is reasoned that this could be caused by the power plant control system (through achieving decoupling). Hence, is chosen that there is no feed through in this loop ($tf = 0$).

When the identification procedure is finished, 16 separate transfer function data sets have been obtained. These transfer functions are not immediately usable as linear model, first some post-processing is required. All transfer functions data sets are exported from IDENT as IDPOLY data sets. These are linear polynomial discrete input-output models. To transform IDPOLY into standard usable format, all 16 sets are transformed into discrete state spaces (by using the tool SS on the IDPOLY object).

Finally to obtain continuous-time transfer functions all state-spaces are converted using the Matlab-tool D2C. No specific conversion method (e.g. tustin or zoh) is selected since D2C uses the information of the data set to determine the correct method. To check that D2C-conversion did not alter model dynamics, the frequency response of the discrete- and continuous-time model are compared. Comparison indicates that the conversion was correct (there was almost complete overlap).

The required 16 continuous-time transfer functions (from: Pvv_{ref}, Tsh_{ref}, $Nbal_{ref}$ and dP_{ref} to: Pvv, Tsh, $Nbal$ and dP) have been obtained (see Table A-1) which correspond to the following $4x4$ model structure (Equation 2-1):

$$y = Gu; \qquad G = \begin{bmatrix} G_{11} & G_{12} & G_{13} & G_{14} \\ G_{21} & G_{22} & G_{23} & G_{24} \\ G_{31} & G_{32} & G_{33} & G_{34} \\ G_{41} & G_{42} & G_{43} & G_{44} \end{bmatrix} \tag{2-1}$$

In Equation 2-1: y and u are defined as follows:

$$y = \begin{bmatrix} Pvv \\ Tsh \\ Nbal \\ dP \end{bmatrix}; \qquad u = \begin{bmatrix} Pvv_{ref} \\ Tsh_{ref} \\ Nbal_{ref} \\ dP_{ref} \end{bmatrix} \tag{2-2}$$

To combine all 16 transfer functions into a single linear model a simulink model, with the structure shown in Table 2-5, is used. The model is a physical representation of Equation 2-1 and is mainly build to simplify practical implementation, use and understanding of the model.

Operating point

For both linearization and system identification, an (linearization) operating point is required. Operating points specify the value, on a non-linear function (i.e. plant), at which linearization takes place. The produced model linearly approximates the plant around this (operating) point. In practice, operating points are often selected close to the expected operating values of the system [15].

In this study the operating point is motivated by the proposed experiment design. During $Charge_{ref}$-change scenario, the simulator will to operate between a $Charge$ of 131.5 and $100MW$ and it is desired to have a (accurate) linear model for this experiment. We consider maximum power the most complex and important simulator state of $Charge_{ref}$-change scenario. Therefore, $Charge = 131.5MW$ is selected as operating point.

2-4-3 Results

As mentioned earlier, both linearization (LINMOD) and system identification (IDENT) have been applied. Linearization produced various critical errors. These errors have been investigated but it is not clear why these errors occur. Attempts to circumvent (e.g. replace Xsteam) or to solve the errors by remodeling simulator components (e.g. modification of the steam pressure safety valve) did not produce viable solutions. Hence, linearization was not succesfull. However, it was possible to obtain a linear model through system identification.

Application of system identification has produced the following model structure and model order selection (Table 2-4).

	Pvv	Tsh	$Nbal$	dP
Pvv_{ref}	OE221	OE221	OE221	OE331
Tsh_{ref}	N/A	OE221	ARX441	OE441
$Nbal_{ref}$	N/A	N/A	OE221	OE331
dP_{ref}	N/A	N/A	ARX441	OE331

Table 2-4: Model structures and model orders of Mod

The 16 corresponding continuous-time transfer functions are presented in Table A-1. The set of transfer functions that are listed as N/A are the transfer functions which had an exceptionally low signal to noise ratio. It is reasoned that this could caused by the classical control system of the power plant (through achieving decoupling). Based on this reasoning was chosen to define the feed through as 0.

Figures 2-6 to 2-9, illustrate the behavior of the found linear model (Mod) compared to the simulator (Sim), while both undergo excitation by the specified identification signals. These figures indicate that a good model has been found (i.e. there is much overlap between the responses of Sim and Mod).

When all transfer functions are combined into a linear model (as proposed), the following structure is obtained (Table 2-5).

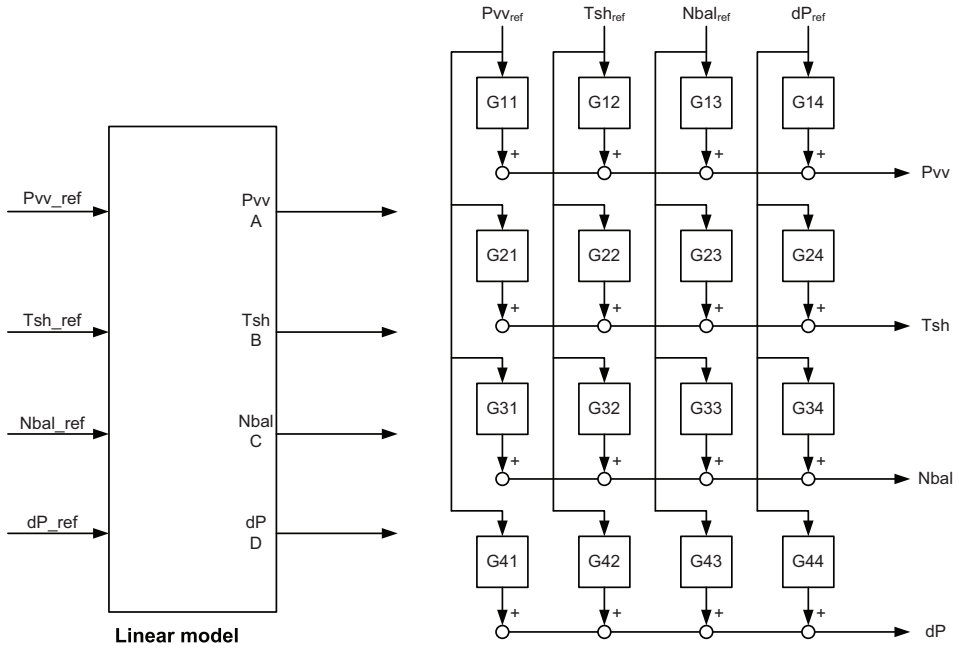

Table 2-5: Linear model: in- and outputs & internals

Note that the found linear model (Mod) is the linear representation of Sim (Figure 2-10) around operating point $Charge = 131.5MW$.

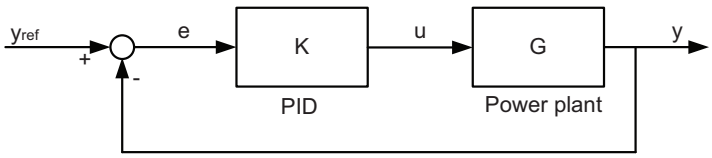

Figure 2-10: Sim (control) structure

Before using Mod for control design, we would like to have an indication on its quality (i.e. how well does Mod describe Sim). The model is considered to have good quality when the difference in behavior (i.e. response) of Mod and Sim is small. To measure this, we would ideally like to compare the responses of Mod and Sim for the specified $35MW$ change of $Charge_{ref}$. However, since Mod does not have an input for $Charge_{ref}$ this is not possible.

When a change of $Charge_{ref}$ takes place in Sim, the PSC (Pressure Setpoint Calculation) module calculates a new value for Pvv_{ref}. As such, a change of $Charge_{ref}$ is for the linear model a change of Pvv_{ref}. Therefore, instead of a change of $Charge_{ref}$, both Mod and Sim are subjected to a change in Pvv_{ref} (while all other conditions remain constant). Their responses are compared and their correspondence is considered to be an indication of the model quality.

To test the correspondence between Mod and Sim (in the selected operating range), Pvv_{ref} is stepped-down (amplitude: $7bar$) from its initial value ($136bar$). After $4000s$ Pvv_{ref} is stepped back to its initial value. The following response is obtained (Figure 2-11):

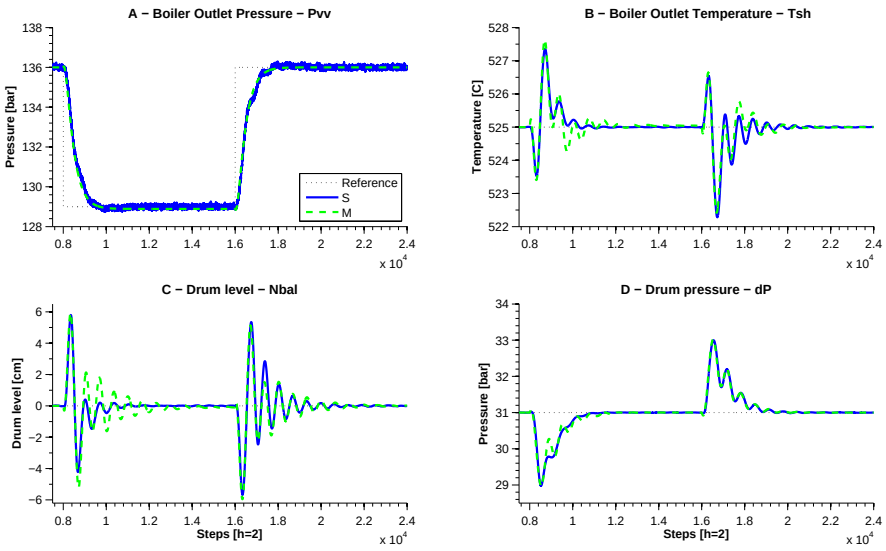

Figure 2-11: Validation of Mod: Compare Plant Output responses of Sim and Mod

In Figure 2-11 is seen that Mod estimates the behavior of the actual Pvv- and dP-loop quite well (i.e. the response of Sim and Mod almost completely overlap each other). The estimation of the actual Tsh- and $Nbal$-loop behavior is satisfactory (i.e. Mod overlaps the behavior of Sim for a large part). However, oscillations (observed) in these loops are somewhat bigger or less damped in Mod. Hence, for these loops the to-be-designed H_∞-controller expects worse behavior than necessary. Since this is only a small difference, it is expected that this will not be a big problem (especially when including robustness criteria in the control design). Therefore, is concluded that Mod is acceptable for control design.

To prevent numerical-errors during control design, Mod has been balanced and placed into minimal realization (using Matlab-functions SSBAL and MINREAL). After this, the frequency response of the balanced Mod is compared to the orininal Mod. The responses indicate that no important dynamics have been lost (5 states were removed but the two responses overlapped completely).

2-5 Conclusion

In this chapter the Laborelec simulator (Section 2-1) has been modified for research of the problem statement (Section 1-3). Furthermore, the modified simulator (Sim) is used to derive a linear model (Mod, Section 2-4).

Chapter 3

Improving Performance with Advanced Process Control

In this Chapter, a brief introduction of the to-be-implemented control design is given. Hereafter, the used control method (H_∞-control) is described shortly (Section 3-2). After this, two possible methods to design the H_∞-controller (i.e. weight design methods) are discussed (Section 3-3). The observations and results of each method are discussed (Section 3-4) and finally the conclusions on power plant control are presented in Section 3-5.

3-1 Introduction

In this chapter the H_∞-controller (K_{H_∞}) is synthesized. To compute K_{H_∞}, the H_∞-control-algorithm uses linear model Mod (also denoted by G) and a performance objective.

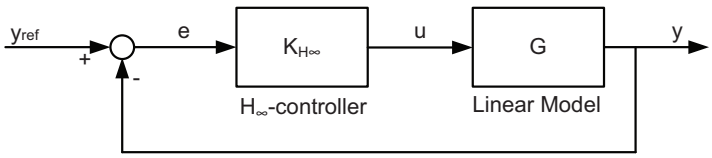

Figure 3-1: Schematic: proposed H_∞-control-structure

The performance objective is designed through an iterative procedure of 4 steps. First, a controller is computed using a reasonable initial (guessed) performance objective (Section 3-3). The found controller is applied to the linear model (Figure 3-1) resulting in the proposed master (H_∞) - slave (PID) structure (G is already PID-controlled). Hereafter, the H_∞-controlled Mod (i.e. Mod_{H_∞}) is subjected to a specific scenario (Section 3-3) and the performance of the controller (i.e. settling time, rise time, oscillation amplitude and steady state offset) is evaluated.

Finally, based on observed control performance, the performance objective is tuned (i.e. loop shaping) until the point is reached that stricter performance objectives do not improve performance.

When the design procedure is concluded, the obtained H_∞-controller is applied to Sim (Figure 1-5). In this setting the controller performance is evaluated on a power plant simulator (the simulator behavior is considered equal to that of a power plant).

3-2 H_∞-control

In general, control design problems are formulated as follows: find a controller K that minimizes the difference between the desired plant behavior and the plant output [17]. In H_∞-control [14] this is done as follows.

The H_∞-control-algorithm computes a stabilizing H_∞-optimal state space controller K_{H_∞} (a MIMO transfer function matrix), which achieves that MIMO transfer function matrix N satisfies:
$||N||_\infty < 1$

N consists of certain selected closed-loop transfer function matrices (e.g. S and KS) and weighting transfer function matrices (e.g. W_p and W_u). This combination defines N as a closed-loop performance objective matrix, which is to be made small through feedback. The controller, produced with the H_∞-algorithm, shapes the closed-loop plant behavior according to the defined weights. Hence, the difference between the desired plant behavior and output has become small.

In other words, through designing weights it is possible to find a controller that shapes the behavior of Mod "according to our requirements". The choice of requirements is not completely free, there are limitations. The different limitations, on design of an H_∞-controller for MIMO plants or on control of MIMO plants in general, are extensively addressed in [4]. Furthermore, for a detailed description of the H_∞-control-algorithm please refer to [4, 15].

As discussed above, the H_∞-algorithm uses performance objective (N) to compute H_∞-controllers. Furthermore, it is required that N is formulated in the generalized plant P structure.

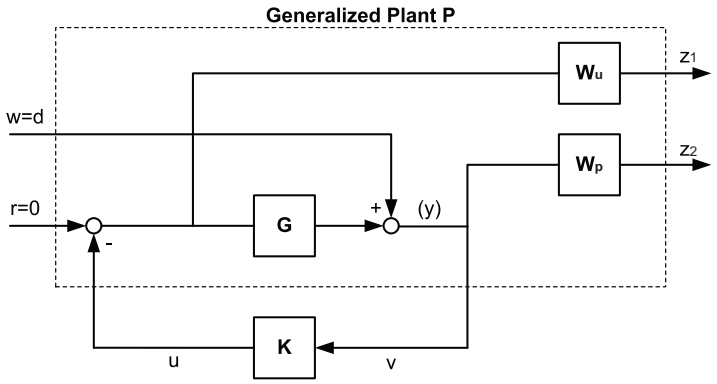

Figure 3-2: Generalized Plant structure

In the generalized plant structure (Figure 3-2), Mod and performance demands (in the form of weighting functions) are defined explicitly together. As an example, in Figure 3-2, weights have been imposed on the sensitivity function S $(= (I + GK)^{-1})$ through W_p and control sensitivity KS (through W_u). Note that controller K is not inside generalized plant P, this structure is required to calculate and optimize K iteratively.

The following equations describe the generalized plant structure:

$$\begin{bmatrix} z \\ v \end{bmatrix} = \begin{bmatrix} P_{11} & P_{12} \\ P_{21} & P_{22} \end{bmatrix} \begin{bmatrix} w \\ u \end{bmatrix} \tag{3-1}$$

Such that:

$$z = \begin{bmatrix} W_p S \\ W_u K S \end{bmatrix} w \tag{3-2}$$

$$u = K(s)v \tag{3-3}$$

Where:

- z the output ("error") signals to be minimized.
- w disturbances on the plant (i.e d).
- v measurements into the controller.
- u control signals into the plant.

Furthermore, the generalized plant structure and its requirements, for H_∞-synthesis, are extensively documented in [4].

The method, used to design the weights (i.e. shaping the performance objective), is discussed in the approach (Section 1-4). In this procedure, the main objectives are to find an H_∞-controller that achieves decoupling and disturbance rejection. It is reasoned that decoupling can be achieved through specifying weights in a diagonal matrix format. This emphasizes that the off-diagonal terms (i.e. coupling) are required to be zero. Furthermore, was reasoned that full decoupling is probably not completely possible (theory vs. practice and off-diagonal terms are very small but not zero, see Equation 3-8). Therefore, is expected that some coupling effects will continue to influence the processes loops. Considering that this is combined with the disturbing influence of throughput changes, it is reasoned that disturbance rejection could improve loop performance. Hence, the S/KS design is used as performance objective. Indeed, performance weight (W_p) and control weight (W_u) are implemented. These weights are both MIMO and are 4x4 diagonal matrices (see Equation 3-4).

$$W_p = \begin{bmatrix} w_{p1} & 0 & 0 & 0 \\ 0 & w_{p2} & 0 & 0 \\ 0 & 0 & w_{p3} & 0 \\ 0 & 0 & 0 & w_{p4} \end{bmatrix}; \qquad W_u = \begin{bmatrix} w_{u1} & 0 & 0 & 0 \\ 0 & w_{u2} & 0 & 0 \\ 0 & 0 & w_{u3} & 0 \\ 0 & 0 & 0 & w_{u4} \end{bmatrix} \tag{3-4}$$

More specifically shaping the loop of S improves amongst others the closed loop disturbance rejection performance (since $y = Sd$). Shaping the loop of KS reduces the input usage (i.e. control energy) by the controller, hence requiring the controller to be more efficient with the available actuation power. Furthermore, KS is important to achieve robust stability. A detailed specification of the control properties of S and KS is found in [4].

Hence, the H_∞-algorithm is to find a stabilizing controller that achieves or minimizes:

$$\left\| \begin{matrix} W_p S \\ W_u K S \end{matrix} \right\|_\infty < 1 \tag{3-5}$$

This suppresses or minimizes the gain in the worst-case direction, and frequency, of the performance objective N. In other words, the maximum (frequency-dependent) singular value of each transfer function is to be minimized (for full detail refer to [4]).

As Equation 3-4 shows, W_p and W_u are composed of 4 weighting transfer functions each (one per loop). Each of these weighting functions ($w_{p1,\ldots,p4}$ and $w_{u1,\ldots,u4}$) is tuned through an iterative procedure (Section 3-3).

Robustness

An important aspect of H_∞-control design is robustness. The H_∞-controller is based on linear model G, which is an estimation of power plant simulator Sim. However, due to for example nelected or unmodelled dynamics, G never exactly represents the actual plant. To equip the controller for these kind of uncertainties, robustness criteria are included in the control design. Robustness criteria, describe how the controller should behave under uncertain situations. There are two main robustness criteria: the ability of the controller to remain stable (robust stability, RS) and the ability of the controller to perform according to (our) specifications (robust performance, RP) under uncertainty.

In [4] is documented how robustness criteria are implemented (i.e. robust control design) and evaluated for both SISO- and MIMO-control systems. For design of robust MIMO-controllers it is required to exactly define the uncertain parameters of nominal plant G (i.e. Mod). Since, we can say little about uncertainty of the linear model parameters it is not usefull to design the H_∞-controller using these rules. Instead, an alternative procedure is followed. To keep an eye on robustness during H_∞-control design, following SISO-criteria are evaluated for each loop separately (Equations 3-7, a full detail description of these criteria is given in [4]).

$$|S| < 1/|w_p| \text{ and } |KS| < 1/|w_u| \tag{3-6}$$

Furthermore, the designed H_∞-controller is by definition stable for the nominal plant (i.e. nominal stability, because the H_∞-algorithm only produces stable controllers). Furthermore, through weight design it also has good performance on the nominal plant (i.e. nominal performance). However, this combined with evaluation of the SISO-robustness criteria does not guarantee robustness. Hence an additional test is required. Note: not fulfilling the SISO-robustness criteria does indicate robustness issues for the MIMO-case.

Nominal plant G is derived from power plant simulator Sim and the difference between these two is actually the exact but unknown of uncertainty. Therefore it is reasoned that, the simulator may be considered as uncertain plant G_p (in which nominal plant G is combined with uncertainty Δ). Hence, it is reasoned that we can test robust stability and robust performance by application of the H_∞-controller to Sim.

Formulating this test into criteria: robust stability is achieved when H_∞-controller is stable on Sim and robust performance is achieved when the H_∞-controlled Sim performs better than without H_∞-control.

H_∞-algorithm
In practice H_∞-controllers are found using the H_∞ sub-optimal control problem formulation: given $\gamma > \gamma_{min}$, find all stabilizing controllers K_{H_∞} such that

$$||F_l(P, K)||_\infty < \gamma \tag{3-7}$$

This can be solved efficiently using the algorithm of [18]. By reducing the H_∞-norm iteratively, through changing K, an optimal solution (controller) is approached.

To find solutions, the algorithm solves two Ricatti equations. Furthermore, the controller will have the same state-dimension as plant P. Note that in this representation P is the generalized plant, K is K_{H_∞}, γ is the minimum H_∞ norm-value that indicates that the solution (i.e. controller) is sufficiently (sub)optimal and $F_l(P, K)$ is the linear fractional transformation of the plant and controller.

Controller-order
To prevent numerical-errors and to improve its practical applicability, it is desired to reduce the controller-order (i.e. the order of found K_{H_∞}) as much as possible (i.e. without losing model dynamics). Furthermore, low-order models are often easier to analyze and much faster to simulate. Therefore, the K_{H_∞}-order has been reduced with Matlab-function: REDUCE (a Hankel singular value based reduction algorithm). Using this tool the controller-order has been reduced from 39 to 15. To confirm that the reduction did not result in dynamics loss, the frequency response of both the high- and low-order H_∞-controller have been compared. This confirmed that there was no dynamics loss (complete overlap). After this only the low-order K_{H_∞} is used.

3-3 Methods

Designing weights for H_∞-synthesis is the procedure of translating control objectives into weigths that achieve them. As previously defined, weights W_p and W_u are used. This will produce the following closed-loop performance objective matrices:

$$\begin{bmatrix} w_{p1} & 0 & 0 & 0 \\ 0 & w_{p2} & 0 & 0 \\ 0 & 0 & w_{p3} & 0 \\ 0 & 0 & 0 & w_{p4} \end{bmatrix} \begin{bmatrix} S_{11} & S_{12} & S_{13} & S_{14} \\ S_{21} & S_{22} & S_{23} & S_{24} \\ S_{31} & S_{32} & S_{33} & S_{34} \\ S_{41} & S_{42} & S_{43} & S_{44} \end{bmatrix} = \begin{bmatrix} w_{p1}S_{11} & w_{p1}S_{12} & w_{p1}S_{13} & w_{p1}S_{14} \\ w_{p2}S_{21} & w_{p2}S_{22} & w_{p2}S_{23} & w_{p2}S_{24} \\ w_{p3}S_{31} & w_{p3}S_{32} & w_{p3}S_{33} & w_{p3}S_{34} \\ w_{p4}S_{41} & w_{p4}S_{42} & w_{p4}S_{43} & w_{p4}S_{44} \end{bmatrix} \tag{3-8}$$

Note: the same applies to W_u combined with KS.

In which $w_{p1,\ldots,p4}$ and $w_{u1,\ldots,u4}$ are each designed individually using the methods described below. Furthermore, their control objective is reducing oscillations in and increasing control performance of the chosen process variables (Pvv, Tsh, $Nbal$ and dP). Also is required that the controller should be robustly stable and performing as defined.

Method 1: the general weight design method

To translate our 'requirements' into weights we can use the general weight design method [4] which provides a fixed framework for the control design task. The framework allows the design task, through the definition of a set of basic performance requirements, to be simplified into the selection of a set of minimum bandwidth frequencies (ω_b) for the W_p transfer functions ($w_{p1,\ldots,p4}$). This is achieved by assigning every W_u transfer function a very low value and defining each w_p as Equation 3-9:

$$w_p = \frac{1/M_p \cdot s + \omega_b}{s + \omega_b A} \tag{3-9}$$

Where:

M_p = maximum peak magnitude of S
ω_b = minimum bandwidth frequency
A = maximum steady state tracking error (i.e. static-gain)

Assigning low values to each w_u (e.g. $w_u = 0.0001$, "unconstrainded" control effort) allows to design a controller by only considering the control performance (the shape of S through w_p). When w_p is designed, robustness is introduced by shaping the control sensitivity (KS) through w_u. Defining w_u limits amongst others the size and bandwidth of the controller, hence the used control energy (ensuring efficient control).

The initial values of M_p and A are directly specified with basic performance requirements. Specification of maximum peak magnitude M_p prevents amplification of noise at high frequencies and also introduces a margin of robustness, typically $M_p = 2$, hence this is the initial value for M_p. Through specification of A the integrating action is determined, hence the maximum steady-state error. To achieve (near) integral action $A = 10^{-4}$ is typically selected ($A \neq 0$ because then the weight is not bi-proper, which causes numerical errors).

ω_b is selected through an iterative process in which, for every value of ω_b, an H_∞-controller is synthesized and applied to the linear model. An alternative $Charge_{ref}$-change scenario (see Section 3-4-2) is applied to the controlled linear model, and its response is observed. As initial choice, ω_b is often given a very low value ($\omega_b = 0.0001$). This requires a very low performance of the H_∞-controller, resulting in very high settling times, no overshoot and generally small oscillations in Pvv, Tsh, $Nbal$ and dP. Then ω_b is increased as much as possible, while observing the settling time, overshoot, and oscillation in each process loop. The procedure stops when ω_b achieves the lowest settling time and overoot, while there is still almost no oscillation (a little oscillation is acceptable). Increasing ω_b even further would decrease performance again. This is a loop-shaping procedure based on time-domain behavior.

As a 'maximum' ω_b is found for selected values of M_p and A it is possible to improve performance even further by fine-tuning. Fine-tuning concerns small increase of M_p which, in case that M_p limits perfomance, allows further increase of ω_b. The desired value of M_p and ω_b is selected based on trade-off between achieved the settling time, overshoot, and decoupling in each process loop. Instead, it is sometimes favorable to decrease M_p (for the found 'maximum' ω_b) to trade-off between settling time and overshoot. Since each loop has its own dynamics, the complete design procedure is caried out for each loop (i.e. $w_{p1,\ldots,p4}$) separately. Hence, four performance weights are produced.

After designing w_p, a similar approach is followed for the design of the four w_u. First a very small value of w_u is selected (e.g. $w_u = 0.0001$) and then it is increased as much as possible. Note that these weights are constant for all frequencies, hence KS stays below this value but no additional shaping is done. To allow tight control at low frequencies, while achieving sufficient roll-off in high frequencies and also robustness, it is better to use a low-pass filter (its bandwidth will then determine the closed-loop bandwidth). In this case also KS is shaped but the weight design is more complex.

Note that by changing the design of W_p also the shape of KS is influenced. Hence, the design of W_p and W_u are related. Indeed when designing W_p, for a very small W_u, as strict as possible (i.e. increasing the performance requirement until the point that no stable controllers can be found) it is impossible to define strickter W_u afterwards. However, when this procedure is done for a reasonable W_u, the performance requirement can be made strict again only now W_u is already reasonable. The sence of reasonable weights is formed in a few design cycles. Then is known which ranges for W_u / W_p are possible and which combinations lead to reasonable performance when the H_∞-controller is applied to Mod.

Method 2: constrained weight design

As the results section will show, the general design method is not applicable to all systems. The "unconstrained" control effort will result in unstabilizing controllers (i.e. the H_∞-controller destabilizes Sim) and it is impossible to evaluate the cause. Although unresearched, most reasonable explanation is that the master-slave (i.e. H_∞-PID) setup reveals a high input sensitivity of the simulator and actions of the H_∞-controller destabilize the simulator. However, cause could also be model uncertainty which requires very robust controllers (starting at $w_{u1,\ldots,u4} = 0.0001$ directly results in unstabilizing controllers) to obtain reasonable performance. Method 2 circumvents this issue by shaping the KS-loop first (i.e. selecting a reasonable W_u). Hence, the same procedure (as Method 1) is followed only starting with the design of W_u.

3-4 Results

During the actual control design task, the parameters of the H_∞-controller are iteratively selected using the general or the constrained weight design method. After each selection step, the found H_∞-controller is applied to Mod (i.e. Mod_{H_∞}) and the behavior of the four process variables are evaluated on oscillation reduction and performance increase. At the point where changes in the controller parameters no longer improve these criteria, the final control design is found. In the first part of this section (Subsection 3-4-1), the final control design and the motivation behind the selected parameters is given. In the same way as the iterative selection procedure, the performance of the final control design is evaluated in the experimental setup (Subsection 3-4-2). This is the last evaluation of the controller in the experimental environment.

When the final controller displays good performance in the experimental setup, the control design task is complete. To show that this is a viable control design method and to research how the final controller operates in the power plant simulator (i.e. Sim), the last part of this section (Subsection 3-4-3) evaluates the behavior of Sim when it is modified with the found H_∞-controller (i.e. Sim_{H_∞}). This will provide data on the research questions and provide information on the robustness of the controller. Moreover the difference between the initial and the H_∞-controlled power plant simulator will be made clear.

3-4-1 Designing the H_∞-controller

Use of the general weight design method produces unstabilizing controllers. Future research should adress this issue, however since this is not a main topic of this research the constrained weight design method is applied instead. First step is to specify control sensitivity KS. During preliminary experiments (to explore the range of possible W_u / W_p) was observed that for $w_{u1,\ldots,u4} \leq 0.1$ nominal stable (NS) controllers can be found (i.e. for constant valued-$w_u > 0.1$ the H_∞-algorithm does not find controllers). Hence, an upper value for W_u is found.

For W_u in which $w_{u1,\ldots,u4} = 0.1$, substantial performance requirements (w_p's with $A = 10^{-4}$, $M_p = 2$ and "high" values of ω_b) can be defined. The resulting controllers performed well on the linear model. However during tests on the modified simulator, the well-performing controllers proved to be insufficiently robust (oscillations resulted in instability). Although unresearched, two possible explanations could be that the H_∞-controller starts reacting on noise (which is typically a high frequency phenomenon) or that the controller tries to control the (very) fast loops ($Nbal$ and dP) through the slow loops (Pvv and Tsh). This is a topic that needs further adressing in future research. As solution, the following low-pass filter is proposed:

$$w_{u1,\ldots,u4} = 0.1 \cdot \frac{s+1}{0.04 \cdot s + 1} \tag{3-10}$$

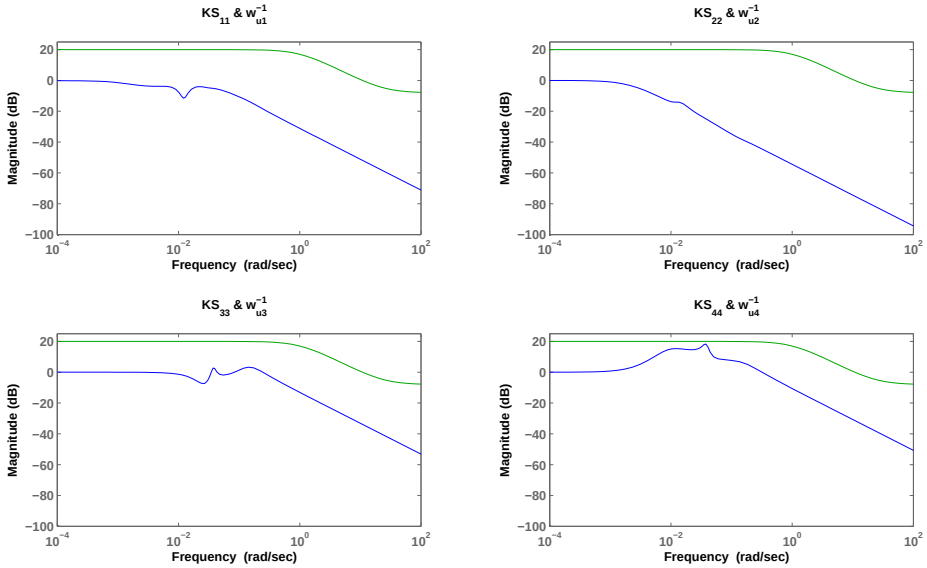

Figure 3-3: Control Sensitivity KS & $w^{-1}_{u1,\ldots,u4}$ of the 4 process loops (Pvv, Tsh, $Nbal$ and dP)

This weight (Equation 3-10 and Figure 3-3) implements a low-pass constraint. In practice this ensures that the designed controller has sufficient power in the low frequencies for disturbance rejection (plant disturbances typically take place in low frequencies). The low-pass bandwidth is $0.5rad/s$ and after this there is a roll-off of about $20dB/dec$. All elements of W_u have the same shape. This is motivated by the fact that individually tuning each element ($w_{u1,\ldots,u4}$) proved to have almost no improving effect on the controller behavior.

The control sensitivity (KS) frequency response (Figure 3-3) indicates that controller K ($= K_{H_\infty}$) easily fullfills weights w_{u1} to w_{u4}. This is reflected by the difference in magnitude of W_u and KS. The reason for this is the followed weight design procedure. However, KS clearly follows the shape of W_u, displaying the same roll-off of about $20dB/dec$. Hence, the W_u requirements have been implemented in the controller. Note that KS_{11} to KS_{44} represent the behavior of the 4 process loops (Pvv, Tsh, $Nbal$ and dP).

After selection of W_u, performance weight W_p is designed. The following performance weights (Table: 3-1 and Figure: 3-4) are found when the proposed tuning method is followed:

	w_{p1}	w_{p2}	w_{p3}	w_{p4}
M_p	1.2	2	2	2
ω_b	0.0015	0.001	0.03	0.03
A	10^{-5}	10^{-5}	10^{-5}	10^{-5}

Table 3-1: Final selection of Performance Weights

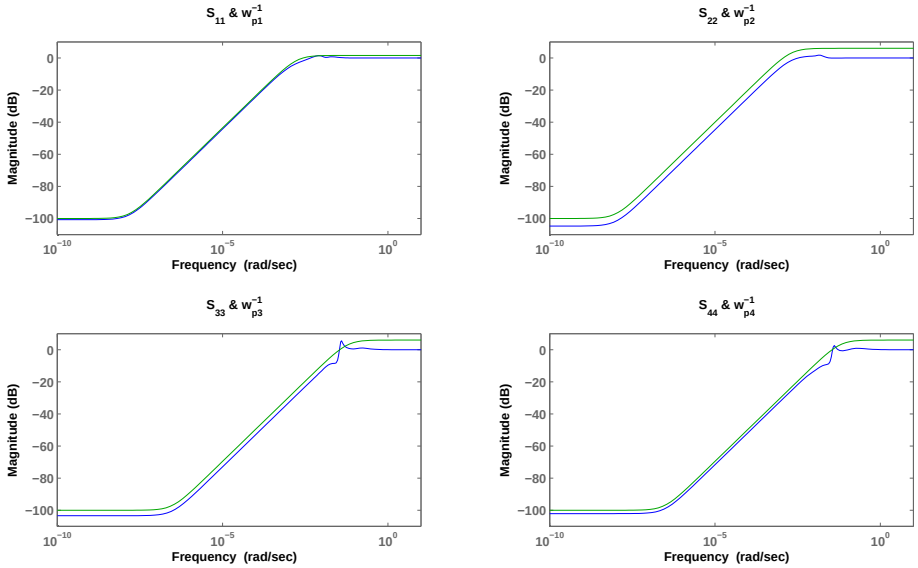

Figure 3-4: Sensitivity S & $w_{p1,\ldots,p4}^{-1}$ of the 4 process loops (Pvv, Tsh, $Nbal$ and dP)

As reflected by Table 3-1, the initial selection of $A = 10^{-4}$ and $M_p = 2$ (for each weight) was very successful. ω_b has been increased as much as possible (indicated by the thight fit between $S_{11,\ldots,44}$ and $w_{p1,\ldots,p4}^{-1}$ in Figure 3-4), while keeping the overshoot limited and the decoupling good. Separate tuning for each loop has resulted in the above shown values, note that $A = 10^{-4}$ is selected for all weights. During fine-tuning was found that decreasing M_p for w_{p1} results in smoother responses and less oscillations in the other loops.

To show the result of the control design, the resulting H_∞-controller is applied to linear model Mod (as shown in Figure 3-1). This combination is called: Mod_{H_∞}. Note that linear model Mod ($= G$) is the linear representation of the PID controlled power plant (hence it is already controlled).

3-4-2 Evaluating the H_∞-controller

To evaluate the behavior of the H_∞-controller, more specifically to compare its behavior to that of the (original) PID control system (represented by Mod), the behavior of Mod_{H_∞} and Mod should be evaluated through a change in $Charge_{ref}$. However, both models only have the inputs: Pvv_{ref}, Tsh_{ref}, $Nbal_{ref}$ and dP_{ref}. Hence, it is not possible to simulate a change in $Charge_{ref}$ the way it is done in Sim. Instead, the following alternative approach is proposed.

In Sim, when $Charge_{ref}$ changes, the PSC (Pressure Setpoint Calculation module) calculates a new (changed) reference for Pvv_{ref} (see Figure 1-4). This results in the response, of the 4 considered process loops, that is under research. Hence, for both Mod and Mod_{H_∞}, a change in $Charge_{ref}$ can be simulated through a change of Pvv_{ref}. During this change, like in Sim, the other references (Tsh_{ref}, $Nbal_{ref}$ and dP_{ref}) remain constant and the 4 outputs are measured.

The proposed alternative (scenario) is implemented as a step down ($7bar$) of Pvv_{ref} after $4000s$. After another $4000s$ (simulation time = $8000s$) Pvv_{ref} returns to its initial value (of $136bar$). A step (shaped) signal is used to accentuate the differences between Mod and Mod_{H_∞} (especially for the Pvv-loop).

Running the proposed alternative scenario results in the following response (Figure 3-5):

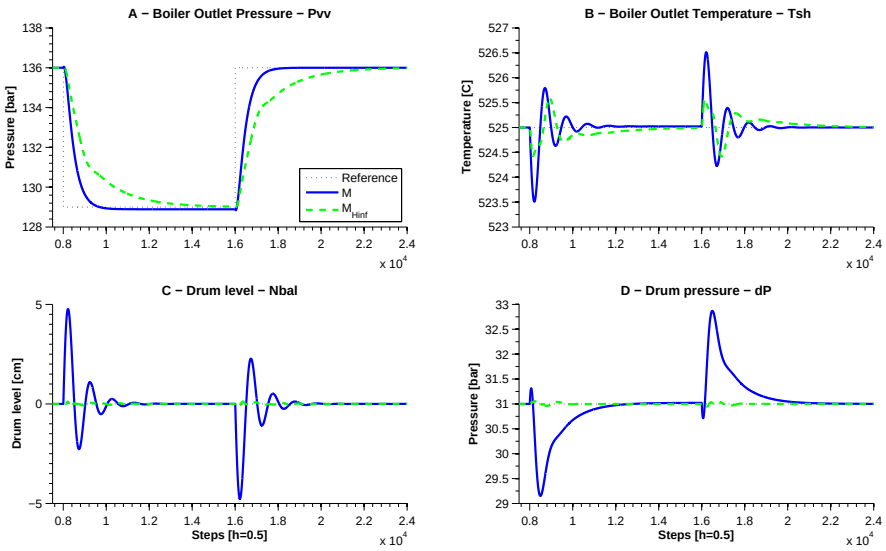

Figure 3-5: Mod controlled with and without H_∞-control: Plant Output

To measure the influence of the designed controller, responses of both the model with (Mod_{H_∞}) and without (Mod) H_∞-controller are shown in Figure 3-5. Now comparing the two, three observations are made:

1. Mod_{H_∞} seems to operate normally (settles to references), it shows roughly the same behavior as Mod.
2. The Pvv-loop in Mod_{H_∞} has a larger settling and rise time.
3. The Tsh, $Nbal$ and dP in Mod_{H_∞} all have smaller oscillations and settling times.
4. There is no steady-state offset in the process loops.

The larger settling and rise time of the Pvv-loop in Mod_{H_∞} indicates that the H_∞-controller is slower than the PID-controller. This is a deliberate choice in the design of the H_∞-controller. For this loop a slower tuning (than the PID) is selected because in practice (i.e. Sim or real power plants) Pvv_{ref} is always calculated by the PSC-module. The PSC always gradually changes Pvv_{ref} (i.e. ramp instead of step) to achieve smooth power output responses. In practice, under normal circumstances, step changes of Pvv_{ref} do not occur. Hence, we have chosen to design the H_∞-controller slower for this loop (than the original PID-controller).

By doing this it is possible to trade-off less strict control of Pvv to more strict control of Tsh, $Nbal$ and dP without, in practice when the H_∞-controller is implemented, changing the Pvv-loop performance. Hence, this change is expected to have no negative influence on the performance of the CC system while the control of the internal variables (Tsh, $Nbal$ and dP) has improved (smaller oscillations and settling times). Considering observations (1 to 4) and corresponding argumentation is concluded that the H_∞-controlled model has a better performance than the original PID-controlled model. Furthermore, the decrease in oscillation amplitude indicates that decoupling and disturbance rejection is achieved (perfect decoupling combined with perfect disturbance rejection would mean that there are no oscillations at all).

Based on the fact that the H_∞-controlled Mod (i.e. Mod_{H_∞}) is stable and shows considerable improved performance is concluded that the found H_∞-controller is nominally stable and performing (NS and NP, as defined in [4]).

3-4-3 H_∞-controller on the Power Plant Simulator

Next step is to confirm that this controller also is robustly stable and has robust performance. This is achieved by implementing found H_∞-controller to Sim (as shown in Figure 1-5). The H_∞-controlled Sim is called Sim_{H_∞}. To test its behavior, the defined $Charge_{ref}$ change scenario ($35MW$ ramp change of $Charge_{ref}$, see Section 2-2) is done.

When Sim_{H_∞} is stable for this scenario, the performance of the controller is evaluated and quantified (by comparing Sim to Sim_{H_∞}). This will provide conclusion on robust performance (RP) and the research questions. More specifically, to which extent the H_∞-controller can reduce the oscillations and increase the performance of the process loops (i.e. Pvv, Tsh, $Nbal$ and dP).

Running the defined $Charge_{ref}$-change scenario on both Sim_{H_∞} and Sim produces the following responses (Figures 3-6 and 3-7):

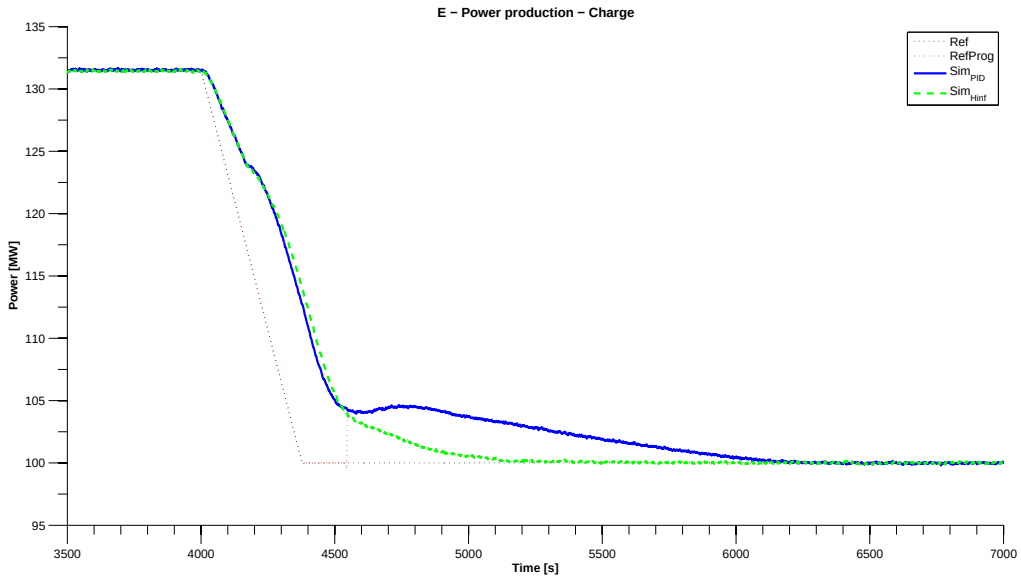

Figure 3-6: Responses of Sim and Sim_{H_∞}: Charge

Analysis of the power production ($Charge$) response (Figure 3-6) leads to the following data:

	$Charge$		
	t_s $[s]$	M_p $[MW]$	t_r $[s]$
Sim	1762	0	1082
Sim_{H_∞}	866	0	526

Table 3-2: Response Analysis: $Charge$

Note that the exact definition of symbols: t_s, M_p and t_r can be found in Appendix B-3.

The response and its analysis are interpreted in the following way: the H_∞-controlled simulator operates as normal (since both responses have the same shape). The rise time (t_r) of Sim_{H_∞} is half of that of Sim, this is achieved through much faster and smoother convergence to its reference value. The settling time (t_s) of Sim_{H_∞} is also cut in half. No overshoot (M_p) and no steady-state error are present. Based on these observations is concluded that the H_∞-controller improves the power production performance.

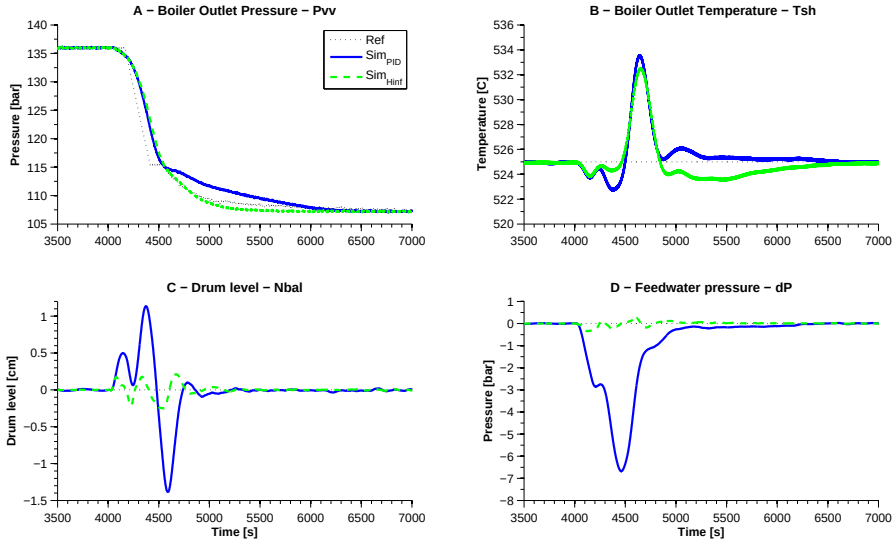

Figure 3-7: Responses of Sim and Sim_{H_∞}: Plant outputs

Analysis of the process variables (Pvv, Tsh, $Nbal$ and dP) response (Figure 3-7) leads to the following data:

	Pvv			Tsh		$Nbal$		dP	
	t_s $[s]$	M_p $[bar]$	t_r $[s]$	t_s $[s]$	M_p $[^\circ C]$	t_s $[s]$	M_p $[cm]$	t_s $[s]$	M_p $[bar]$
Sim	1866	0	1192	2400	10	924	2.5	1358	6.7
Sim_{H_∞}	1084	0	634	2400	8.5	724	0.4	624	0.6

Table 3-3: Response Analysis: Pvv, Tsh, $Nbal$ and dP

The response and its analysis are interpreted in the following way: the smaller (about 40% for both, resp. $558s$ and $782s$) rise- and settling time indicate that the performance of the Sim_{H_∞} boiler pressure loop (Pvv) has increased. No overshoot and steady-state error is present for both simulators. The smaller amplitude (about 75%) in the Sim_{H_∞} drum level loop ($Nbal$) shows that decoupling has been achieved. The smaller settling time (about 20%) also indicates that the performance of the loop has increased. In the Sim_{H_∞} drum pressure loop (dP) decoupling (about 90% lower M_p) is achieved and also the performance has increased (t_s is about 50% lower).

Compared to the other loops in Sim_{H_∞}, the behavior of the boiler output temperature (Tsh) loop has not changed quite as much. The oscillation amplitude has decreased (with about $1.5^\circ C$, which is a decrease of 15%) and the settling time has not changed. Although the improvement is small compared to the other loops, it could have a positive impact. An oscillation amplitude decrease of $1.5^\circ C$ could mean in practice that Tsh_{ref} can be increased with the same amount. A seemingly small increase like this, could safe as much as \$500.000, – (see Appendix C-3) per year on fuel costs for a large power plant.

Due to the higher efficiency also the CO_2- and coolingwater-output could be reduced (both reduce the overall production costs).

However, why the Tsh-loop improves just a little, compared to the other loops, is unknown. There is strong temperature fluctuation in a very short time frame combined with a closed water injection valve (the PID-controller wants to close the valve up till -5%: Figure B-1, Appendix B-1). This could cause integral windup in the H_∞-controller, possibly resulting in a slow response of the H_∞-controller after $4900s$ (observe the H_∞-controller-output: Figure B-3, Appendix B-2). It could also be caused by insufficient capacity of the H_∞-controlled temperature regulation system to compensate for temperature oscillations coming from the low and intermediate stage. The H_∞-controlled temperature regulation system only controls the last stage of the super-heater pack (the pack consists of 3 stages: low, intermediate and high temperature, each with PID-temperature control). Furthermore, strict control of Pvv, $Nbal$ and dP while the Tsh-loop is not completely H_∞-controlled (2 stages are only PID-controlled) could also reduce the performance of the entire Tsh-loop (this could explain the performance difference between the Mod_{H_∞} and Sim_{H_∞} Tsh-loop). However, it could also be caused by model uncertainty, tuning of the PID-controllers in Sim or tuning of the H_∞-controller.

When the difference in the responses, of Sim_{H_∞} and Sim, are considered is concluded that: the H_∞-controller achieves decoupling and increases the performance of the Pvv, $Nbal$ and dP loops. Furthermore, note that perfect decoupling and control performance would fully suppress the oscillations in loops Tsh, $Nbal$ and dP. Hence, perfect decoupling and control performance has not been achieved. However, considering that Sim represents a real life power plant the change in behavior seems promising.

3-5 Conclusion

Summarizing the previous section, H_∞-control has achieved better performance for:
- The charge loop ($Charge$) is twice as fast, with a $896s$ lower settling time.
- The boiler pressure loop (Pvv) is about 40% faster, with a $782s$ lower settling time.
- The drum level loop ($Nbal$) is about 20% faster, with a $200s$ lower settling time.
- The drum pressure (dP) loop is twice as fast, with a $734s$ lower settling time.

Furthermore the H_∞-control has achieved decoupling for:
- The boiler outlet temperature loop (Tsh), with an oscillation amplitude decrease of about 15%.
- The drum level loop ($Nbal$), with an oscillation amplitude decrease of about 75%.
- And the drum pressure loop (dP), with an oscillation amplitude decrease of about 90%.

There are no oscillations in the $Charge$ and Pvv loops.

The increased performance of the $Charge$ and Pvv loop is also reflected by the rise time of these loops, which has decreased with 50%. And finally, based on arguments from practice, is concluded that the performance of Boiler outlet temperature loop (Tsh) is improved by the H_∞-controller (although the unchanged settling time).

Chapter 4

Improving Flexibility with Advanced Process Control

This chapter shows that successful application of MIMO APC for control of internal process variables (Pvv, Tsh, $Nbal$ and dP) also improves overall plant performance.

First, is introduced how improved control of internal process variables can influence the overall plant performance (Section 4-1) followed by a description of the methods used to research this (Section 4-2). The results of the study are presented (Section 4-3) and finally a conclusion is drawn (Section 4-4).

4-1 Introduction

The overall performance of a power plant is defined by two main properties, namely: the efficiency of the power plant and its maximum (power) production rate (MPR).

Energy conversion machines, like power plants, convert input energy (i.e. fuel) into useful output energy (i.e. electric power). Efficiency is the ratio between the amount of input energy and the amount of useful output energy (i.e. how much input energy is converted into useful output energy). This is a useful measure of how much energy is lost or wasted, hence: the overall performance of the process.

The main objective of any power plant is: producing the desired amount of power at the right time. Hence, its ability to fulfill this objective is an important factor when evaluating overall performance. The ability to produce power at the right time is determined by the maximum production rate (MPR) of the power plant (i.e. the maximum rate at which the plant can adapt production). For Les Awirs 4, the MPR is set at $5MW/min$.

The MPR is not necessarily the maximum rate that is physically possible for a plant, moreover the MPR is often defined to keep plant operation costs below a certain level. Increasing the MPR leads to more extreme process conditions (stresses, heat flux, cavitation). This results in more wear, which results in higher operating costs. Furthermore, choosing the MPR too high leads to reduced plant lifetime, reliability and safety. The MPR is defined through trade-off between all these aspects. The production rate at which these risks become unacceptable; is defined as the MPR.

In last chapter was shown that, through H_∞-control, it is possible to improve the control of internal process variables. Also was reasoned that this increases power plant efficiency. Furthermore, reasoning from perspective of the MPR; when H_∞-control is implemented the process conditions become less extreme. Therefore, reducing the (power plant) operating costs that occur when the MPR is $5MW/min$.

In this chapter is researched to which extent the MPR can be raised until the until the same (extreme) process conditions occur (as in the original PID-controlled power plant). This question has not been formulated in the problem statement and it is therefore an additional part to this study. The relevance of this additional part is outlined in the following two paragraphs.

Often it is most attractive to operate power plants under low operating costs (and with high efficiency). However, in some cases (especially for peak-power prices) it is very profitable to produce as much power as fast as possible (peak-production). In this case it is very attractive to raise the MPR (e.g. from $5MW/min$ to $10MW/min$) instead of operating under high(er) efficiency.

It seems that, the results achieved with H_∞-control provide the possibility to trade-off operating costs to MPR (i.e. power plant operators can choose between improving control of internal process variables or increasing MPR). It is reasoned that this could give power producers a new method to optimize profit. Furthermore, power plant operators are contracted to keep a certain amount of MPR available at all times (e.g. $45MW/min$). This is especially profitable during day, since at that moment a much larger amount of MPR is available (almost all power plants are active) and all power is used. During nights however, power producers are obligated to keep power plants in production to fulfill the MPR requirement while only a small amount of power is required which is quite expensive. Should it prove possible to increase the MPR using H_∞-control, the amount of active night power plants can be reduced. This could safe power producers a lot of money while also reducing their environmental footprint. Therefore, this additional research question is included into this study.

4-2 Methods

To study the additional research question, the following two versions of the H_∞-controlled simulator (Figure 1-5) are used. Their structure is completely identical. They only have a different MPR-setting (simulator setting: $Charge$-gradient).

Sim_{H_∞} as used throughout the study (hence: $MPR = 5MW/min$).
$Sim_{H_{\infty,10MW}}$ which is equal to Sim_{H_∞} only now $MPR = 10MW/min$.

Changing the MPR-setting from $5MW/min$ to $10MW/min$ will force the PSC-module (in $Sim_{H_{\infty,10MW}}$) to follow a twice as fast $Charge_{ref}$. To follow this trajectory PSC will also define a steeper Pvv_{ref}. Compared to Sim_{H_∞}, both factors will cause larger oscillations in the process variables (Pvv, Tsh, $Nbal$ and dP) of $Sim_{H_{\infty,10MW}}$. Hence, the process conditions in $Sim_{H_{\infty,10MW}}$ are more extreme than in Sim_{H_∞}. On the other hand however, $Sim_{H_{\infty,10MW}}$ will produce the desired amount of power ($Charge_{ref}$) sooner.

In this experiment Sim, the original PID-controlled power plant, is the standard for operating costs (expressed in process conditions, e.g. oscillation amplitude, settling times). Furthermore, Sim_{H_∞} will show to which extent the process conditions have been improved. Finally, $Sim_{H_{\infty,10MW}}$ will show how much (compared to Sim_{H_∞}) the performance decreases due to the higher MPR-setting.

Each simulator will run the earlier defined $Charge_{ref}$-change scenario. To compare their behavior, the responses of each simulator are shown together in Figures 4-1 and 4-2.

4-3 Results

When the simulation is done, the following responses are obtained (Figures 4-1 and 4-2).

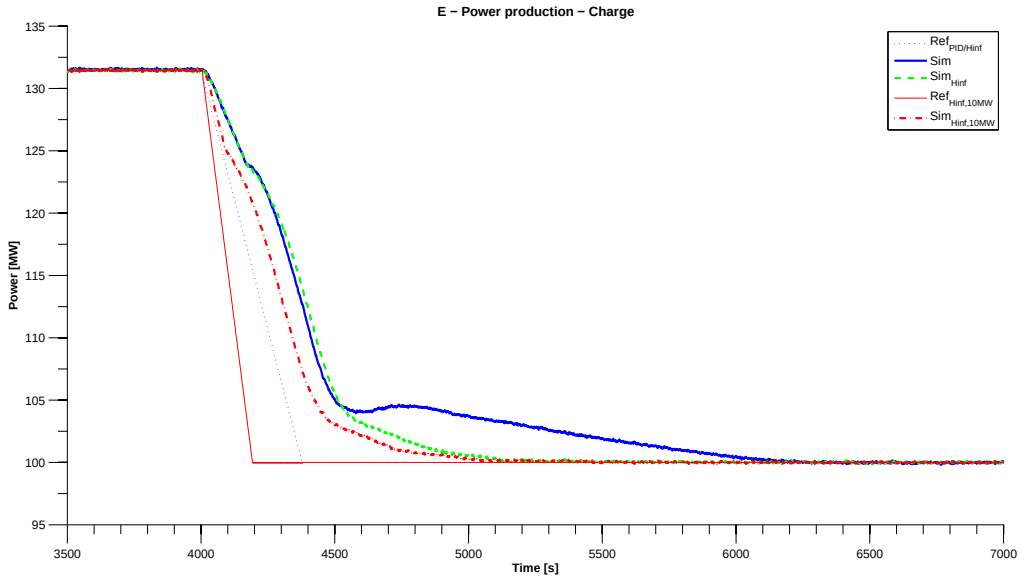

Figure 4-1: Responses of Sim, Sim_{H_∞} and $Sim_{H_{\infty,10MW}}$: Charge

Both Sim and Sim_{H_∞} have the same $Charge_{ref}$-reference (each have an MPR of $5MW/min$). As is seen in Figure 4-1 the $Charge$-responses of Sim and Sim_{H_∞} follow it. Also note that they are somewhat slower than the defined $Charge_{ref}$. As this behavior is already present in Sim, this phenomenon is considered part of normal simulator behavior.

As expected, the $Charge$-response of $Sim_{H_{\infty,10MW}}$ settles faster than the other two. Like for Sim and Sim_{H_∞}, $Sim_{H_{\infty,10MW}}$ is also slower than its defined $Charge_{ref}$. However, it did not become twice as fast. Apparently, doubling the MPR-setting results in an about 25% faster $Charge$-response ($250s$ faster on a total of $1000s$). Nevertheless, comparing the output response (Pvv, Tsh, $Nbal$ and dP) of $Sim_{H_{\infty,10MW}}$ to that of Sim_{H_∞} indicates indeed more extreme process conditions occur.

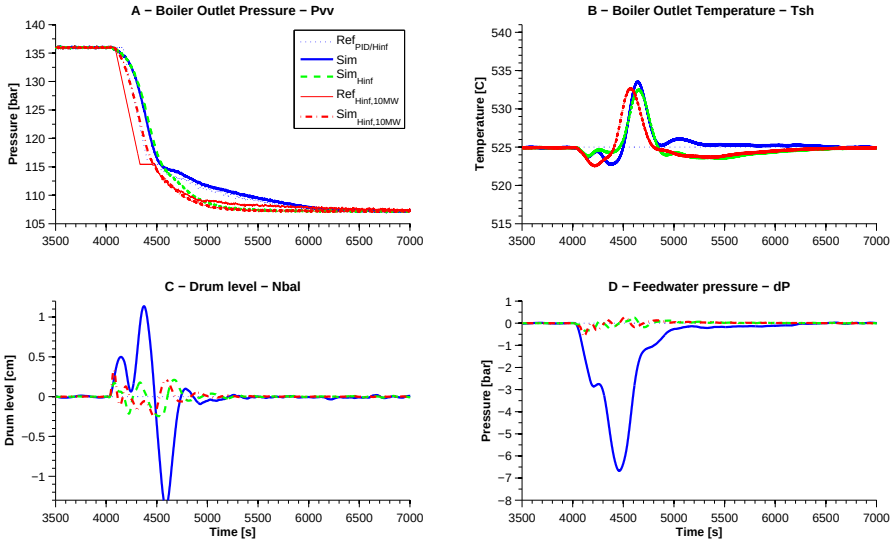

Figure 4-2: Responses of Sim, Sim_{H_∞} and $Sim_{H_{\infty,10MW}}$: Plant outputs

Analysis of the process variables (Pvv, Tsh, $Nbal$ and dP) response (Figure 4-2) leads to the following data:

	Pvv			Tsh		$Nbal$		dP	
	t_s $[s]$	M_p $[bar]$	t_r $[s]$	t_s $[s]$	M_p $[°C]$	t_s $[s]$	M_p $[cm]$	t_s $[s]$	M_p $[bar]$
Sim	1866	0	1192	2400	10	924	2.5	1358	6.7
Sim_{H_∞}	1084	0	634	2400	8.5	724	0.4	624	0.6
$Sim_{H_{\infty,10MW}}$	978	0	592	2276	10	644	0.6	538	0.9

Table 4-1: Response Analysis: Pvv, Tsh, $Nbal$ and dP

The response and its analysis are interpreted in the following way: the $Sim_{H_{\infty,10MW}}$ Pvv-loop has the smallest rise- and settling time which indicates that this loop has the highest performance (compared to Sim_{H_∞} and Sim). In all other loops the settling time has also decreased (compared to Sim_{H_∞} and Sim), hence the controller achieves higher performance for a higher MPR-setting. Interesting to note is that the settling time of Tsh has decreased, indicating increased performance.

Now comparing $Sim_{H_{\infty,10MW}}$ to Sim_{H_∞}, the increased oscillation amplitudes of Tsh, $Nbal$ and dP indeed indicate that the process conditions in $Sim_{H_{\infty,10MW}}$ have become more extreme. However, compared to the initial behavior (i.e. the behavior of Sim) the process conditions in $Sim_{H_{\infty,10MW}}$ are still less extreme (except for Tsh, which has become equal to Sim).

4-4 Conclusion

For the H_∞controlled power plant simulator it is possible to increase the MPR-setting ($10MW/min$ instead of $5MW/min$). Effectively the $Sim_{H_{\infty,10MW}}$ has become 25% faster (instead of twice as fast). As expected this causes more extreme process conditions in $Sim_{H_{\infty,10MW}}$ compared to Sim_{H_∞}. However, when we compare $Sim_{H_{\infty,10MW}}$ to Sim the process conditions are still less extreme (or equal). Based on this is concluded that implementing H_∞-control, next to increasing the power plant efficiency, also creates room to increase the MPR. Hence, improved control of internal process variables also benefits the overall performance.

Chapter 5

Conclusions, Discussion and Future Directions

Concluding remarks are followed by a discussion of the implications of the current investigation, focus will be placed on what is achieved during this study, the expected effects and their importance. Future directions are given at the end of this chapter.

5-1 Conclusions

In this study, an advanced process controller has been designed to improve performance and reduce process variable oscillations in a power plant simulator. It was shown that H_∞-control of boiler output and the feedwater system conditions has resulted in:

- $782s$ ($\approx 40\%$) reduction in the settling time of the boiler pressure (Pvv) loop.
- $200s$ reduction in the drum level ($Nbal$) loop settling time, which is about 20% faster.
- $734s$ ($\approx 50\%$) reduction in the settling time of the drum pressure (dP) loop.

As a consequence, the power output response of the simulator is twice as fast, the $Charge$-loop settling time is $896s$ lower.

With respect to the reduction in oscillations of process variables, the application of H_∞-control has resulted in:

- 15% amplitude decrease in the boiler outlet temperature (Tsh) loop.
- 75% amplitude decrease in the drum level ($Nbal$) loop.
- 90% amplitude decrease in the drum pressure (dP) loop.

There are no oscillations in the $Charge$- and Pvv-loops. Also, the rise time of these loops has increased with about 50%.

It has been demonstrated that improved control of internal process variables also benefits the overall performance. More specifically increasing the effective maximum production rate (MPR) of the H_∞-controlled power plant simulator, with 25%, has a surprisingly small effect on achieved process oscillation and settling time improvement (i.e. reduction) of Sim_{H_∞} (since the process conditions are still less extreme than in the original plant). These findings indicate the possibility to achieve higher power production rates with the same power plant when a H_∞-controller is implemented without increasing the operating costs.

In summary, the current study has led to the development of a H_∞-controller, which is capable of reducing process variable oscillations and increasing the performance of the power plant simulator. Taken together, the present results support the hypothesis that MIMO APC is a viable method in power plant control for attenuation of negative interaction effects.

5-2 Discussion

During this study MIMO APC has been implemented to control the boiler outlet conditions (Pvv and Tsh) and the drum conditions ($Nbal$ and dP) of a power plant simulator. When MIMO APC is applied, oscillations in the boiler outlet and drum conditions are smaller and the settling times are reduced. Furthermore, MIMO APC has been found to successfully suppress the negative influence of the defined $Charge_{ref}$-change.

It has been hypothesized that decreasing oscillation amplitude and settling time lead to an increased overall efficiency of the power plant (Appendix C-3). These effects also reduce power plant wear. Moreover, due to effective suppression of interaction effects the power plant is able to better cope with changes in power demand. These changes give rise to the possibility of increasing the power plant MPR without sacrifice of performance.

Consequently, the power plant will have lower emission of greenhouse gasses and fuel costs. Furthermore, due to decreased wear, the power plant components will have a greater lifetime expectancy while maintenance costs are diminished. The possibility to increase the MPR, allows power plants to be used more flexible. This allows real-time optimization of efficiency, lifetime, emissions and profits.

5-3 Future Directions

Notwithstanding the results of current study, optimization of the H_∞-controller tuning might yield even better performance. Furthermore, evaluation of the practical applicability of the designed H_∞-controller is considered an important starting-point for follow-up studies.

Besides this, the original simulator (Sim_{orig}) displays some unexpected behavior. Therefore, it seems valuable to fully check and document the modeling, the control-system and the parameters of the simulator.

Furthermore, validating the simulator with real-time data would be beneficial. When this is done, an interesting follow-up study could be the research of how this changes the results of the current study.

For future research, viable alternatives to H_∞-control for research of the defined problem statement are: Model Predictive Control and Feed-Forward control (combined with APC). MPC could be a valuable alternative since it designed to deal routinely with equipment- and safety-constraints. Operation at or near these constraints is in many cases necessary to achieve the most profitable or most efficient operation. Given the achieved results, MPC might have the potential to optimize these results. In this study, decoupling is achieved through the design of the H_∞-controller. Instead, it is also possible to achieve decoupling with Feed-Forward control (given the availability of a model with sufficient quality). Combining the achieved decoupling with APC to reduce the effects of throughput (i.e. power output) changes.

Appendix A

Linear Model

To provide more insight into the linear model (Mod, Section 2-4-3) and its properties this appendix will provide a basic property analysis (Appendix A-1).

A-1 Properties of the Linear Model

The linear model (Mod) is a four input, four output model with the following properties:

- Four outputs: the boiler outlet conditions (Pvv, Tsh), the drum level ($Nbal$) and feedwater pressure (dP).
- Four inputs: Pvv_{ref}, Tsh_{ref}, $Nbal_{ref}$, dP_{ref}.

The linear model consists of the following set of transfer functions, which have been found with the system identification procedure:

	Pvv	Tsh	$Nbal$	dP
Pvv_{ref}	$\frac{-1{\cdot}10^{-3}s+9{\cdot}10^{-5}}{s^2+2{\cdot}10^{-2}s+9{\cdot}10^{-5}}$	$\frac{-3{\cdot}10^{-3}s^3+9{\cdot}10^{-5}s^2-4{\cdot}10^{-7}s-7{\cdot}10^{-11}}{s^4+8{\cdot}10^{-3}s^3+4{\cdot}10^{-4}s^2+2{\cdot}10^{-6}s+1{\cdot}10^{-8}}$	$\frac{4{\cdot}10^{-3}s^3-2{\cdot}10^{-4}s^2-2{\cdot}10^{-6}s+4{\cdot}10^{-10}}{s^4+9{\cdot}10^{-3}s^3+5{\cdot}10^{-4}s^2+3{\cdot}10^{-6}s+4{\cdot}10^{-8}}$	$\frac{-5{\cdot}10^{-4}s^5-1{\cdot}10^{-5}s^4+6{\cdot}10^{-7}s^3-1{\cdot}10^{-8}s^2+7{\cdot}10^{-10}s}{s^6+2{\cdot}10^{-2}s^5+1{\cdot}10^{-3}s^4+2{\cdot}10^{-5}s^3+4{\cdot}10^{-7}s^2+3{\cdot}10^{-9}s}$
Tsh_{ref}	0	$\frac{-1{\cdot}10^{-2}s+4{\cdot}10^{-4}}{s^2+2{\cdot}10^{-2}s+4{\cdot}10^{-4}}$	$\frac{-3{\cdot}10^{-3}s^3+2{\cdot}10^{-4}s^2+5{\cdot}10^{-6}s-2{\cdot}10^{-9}}{s^4+2{\cdot}10^{-2}s^3+2{\cdot}10^{-3}s^2+1{\cdot}10^{-5}s+6{\cdot}10^{-7}}$	$\frac{1{\cdot}10^{-3}s^3+8{\cdot}10^{-5}s^2-9{\cdot}10^{-7}s+8{\cdot}10^{-10}}{s^4+4{\cdot}10^{-2}s^3+3{\cdot}10^{-3}s^2+2{\cdot}10^{-5}s+7{\cdot}10^{-7}}$
$Nbal_{ref}$	0	0	$\frac{2{\cdot}10^{-2}s+8{\cdot}10^{-4}}{s^2+2{\cdot}10^{-2}s+8{\cdot}10^{-4}}$	$\frac{-4{\cdot}10^{-2}s^3+8{\cdot}10^{-3}s^2-3{\cdot}10^{-5}s+3{\cdot}10^{-9}}{s^3+3{\cdot}10^{-2}s^2+1{\cdot}10^{-3}s+7{\cdot}10^{-6}}$
dP_{ref}	0	0	$\frac{-3{\cdot}10^{-3}s^3-1{\cdot}10^{-3}s^2-8{\cdot}10^{-6}s+8{\cdot}10^{-9}}{s^4+8{\cdot}10^{-2}s^3+5{\cdot}10^{-3}s^2+1{\cdot}10^{-4}s+2{\cdot}10^{-6}}$	$\frac{4{\cdot}10^{-2}s^2+4{\cdot}10^{-4}s+3{\cdot}10^{-6}}{s^3+0.2s^2+2{\cdot}10^{-3}s+3{\cdot}10^{-6}}$

Table A-1: Linear Model: 4 inputs, 4 outputs = 16 transfer functions

When this set of transfer functions is converted into the generalized plant state-space, a state-space with the following frequency behavior results:

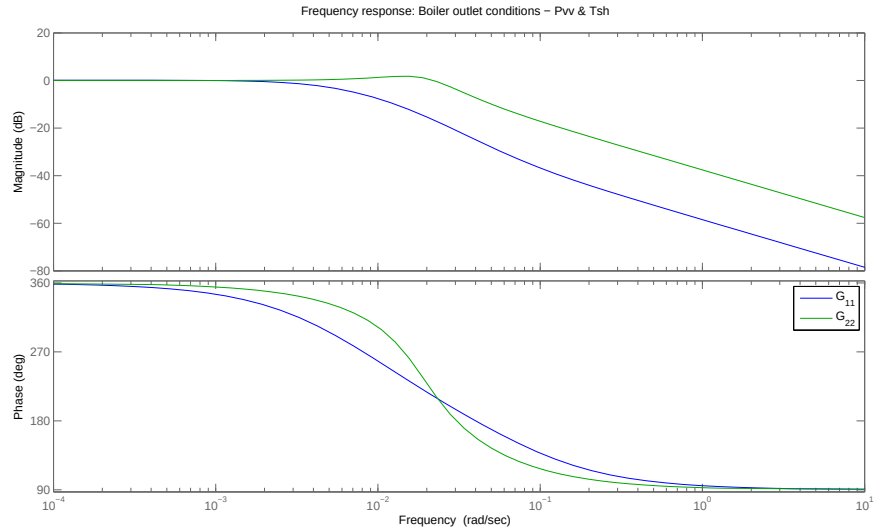

Figure A-1: Frequency response of Mod: Boiler outlet conditions

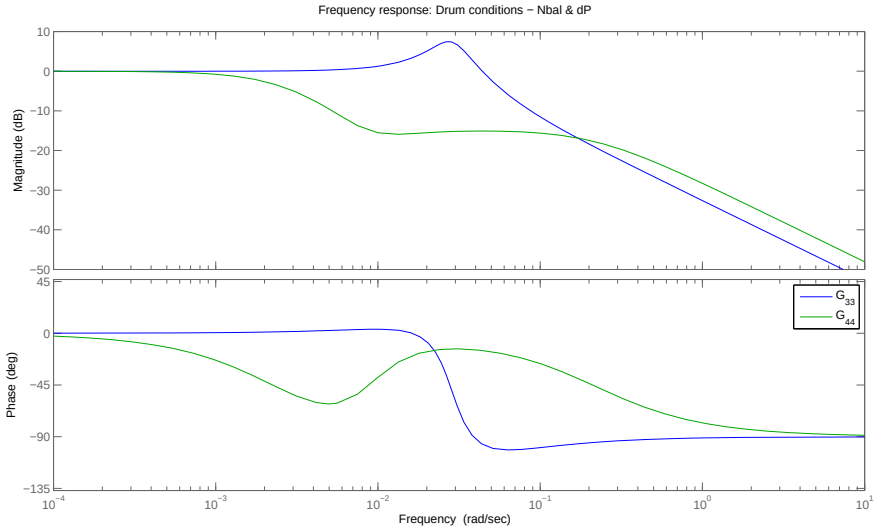

Figure A-2: Frequency response of Mod: Drum conditions

Figures A-1 and A-2 reflect the fact that Mod is already controlled by a tuned PID control system. Quick SISO analysis shows that all loops have excellent phase and gain margins. Point of interest is the resonance peak at $0.028 rad/s$ in the $Nbal$-loop. This peak is probably caused by the integral action of the drum combined with the PID-controller (this should be researched further).

The poles and zeros of Mod are:

$$poles = \begin{bmatrix} -0.006 \\ -0.015 \\ -0.003 \\ -0.006 \\ -0.215 \\ -0.005 \\ -0.002 \\ -0.01 \pm 0.016i \\ -0.003 \pm 0.013i \\ -0.01 \pm 0.026i \\ -0.028 \pm 0.045i \\ -0.008 \pm 0.028i \\ -0.01 \pm 0.040i \\ -0.002 \pm 0.019i \\ -0.003 \pm 0.012i \\ -0.012 \pm 0.033i \\ -0.014 \pm 0.046i \\ -0.003 \pm 0.017i \\ -0.008 \pm 0.012i \end{bmatrix} \qquad zeros = \begin{bmatrix} 8.074 \\ 0.072 \\ 0.0276 \\ -0.025 \\ -0.002 \\ -0.005 \\ -0.046 \pm 0.064i \\ -0.014 \pm 0.046i \\ -0.009 \pm 0.04i \\ -0.006 \pm 0.031i \\ -0.008 \pm 0.025i \\ -0.002 \pm 0.019i \\ -0.004 \pm 0.017i \\ -0.008 \pm 0.012i \\ -0.005 \pm 0.007i \\ -0.003 \pm 0.012i \\ -0.003 \pm 0.013i \end{bmatrix} \tag{A-1}$$

All poles are in the left half plane (LHP). This is as expected, since a power plant is required to be stable under all conditions. However, three zeros are in the right half plane (RHP). The presence of RHP-zeros implicates a limitation on the feedback gain (i.e. performance) when the loop is closed for H_∞-control (for more details please refer to [4]). This is solved by use of the iterative control design method (i.e. the RHP-zeros are part of the maximum achievable performance which is found through iteration).

Since Mod is multivariable, the minimum and maximum singular values of Mod should be analyzed to include the interaction effects. The $\bar{\sigma}$ and $\underline{\sigma}$ of Mod are shown (Figure A-3), and represent the minimum and and maximum gains for any input direction (Mod has 4 inputs).

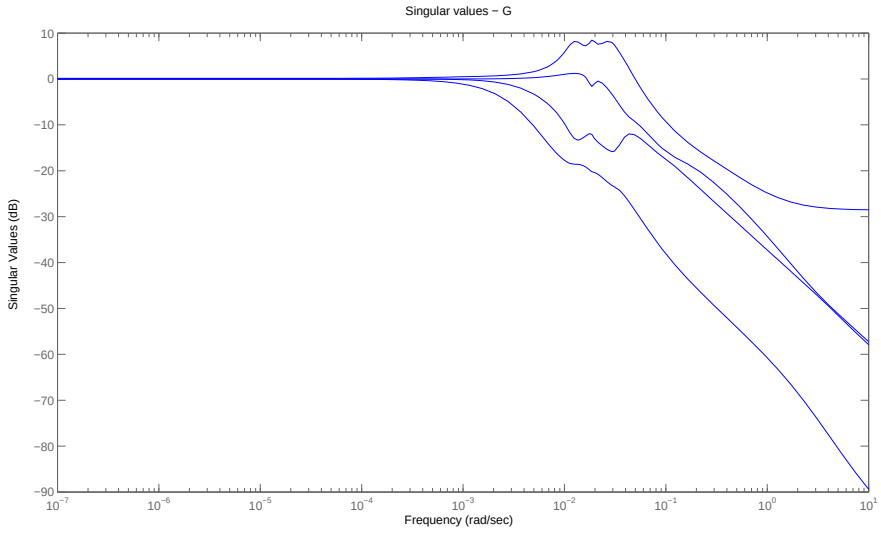

Figure A-3: Singular values of Mod ($\bar{\sigma}$ and $\underline{\sigma}$)

Comparing Figure A-3 to both Figures A-1 and A-2 reveals that they are quite similar. This indicates that there are multivariable effects but that they are not extremely large. Since the power plant (simulator) is already well-controlled this is expected. Furthermore, the (performance) difference between the SISO- and MIMO-response indicates that there is room for improvement (which can be realized by application of MIMO APC). Quick analysis of Figure A-3 shows that the largest peak has a magnitude of about $8dB$ in gain. Hence, for the linear model robustness issues are not expected.

All analysis combined is concluded that the derived linear model is indeed stable. Furthermore, is shown that the PID controllers achieve already quite good performance. However, the present multivariable effects provide plenty of room for improvement. No abnormalities have been detected and it seems that the linear model is viable for use of control design.

Appendix B

Controlled Model

B-1 PID Control Signals

For design of the H_∞-controller linear model Mod is used. Mod is an estimated description of the PID-controlled power plant (i.e. Sim). Using this linear model, the H_∞-controller is designed such that the combination of Mod and the found H_∞-controller is stable (see Figure 3-1). However, since Mod only estimates real plant (Sim) it could be that the actual combination (of Sim and the H_∞-controller, see Figure 1-4) or their interaction is or becomes unstable (caused by for example errors in Mod or too large actuation signals of the H_∞-controller) during the $Charge_{ref}$-change scenario.

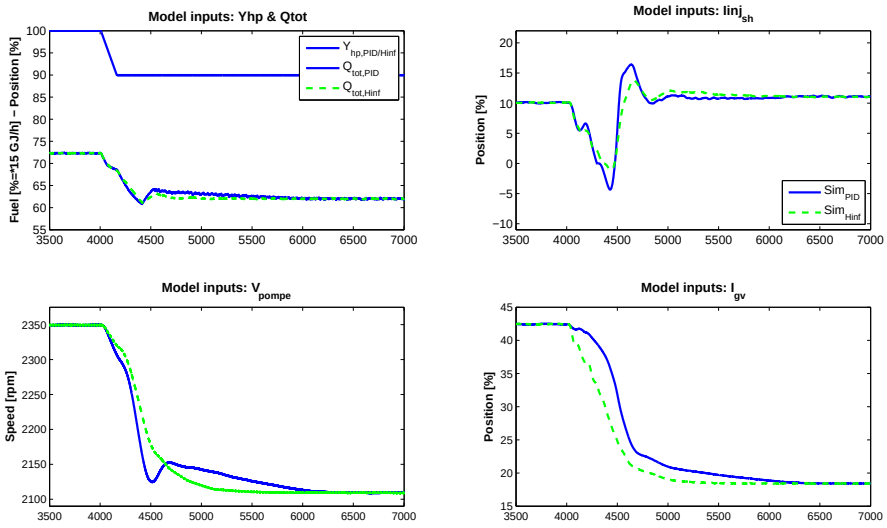

Figure B-1: PID-control signals in Sim_{H_∞}

Since, this could remain hidden inside the connected Sim_{H_∞} (especially if the combination is critically-stable) the behavior (i.e. output, denoted as u in Figure 1-4) of the PID-controllers should be checked. To verify that this is not the case, the PID-control output signals (Q_{tot}, I_{inj}, v_{pump}, I_{valve}, Y_{hp}), which are generated in Sim_{H_∞} during the $Charge_{ref}$-change scenario, are observed (see Figures: B-1 and B-2). Note that PID-controller outputs u are called model inputs, because they are input to the actual power plant model (denoted as G in Figure 1-4).

Figures B-1 and B-2 indicate that the PID-controllers operate normally. This means that presented responses are comparable to those of PID-controllers in the simulator without H_∞-control. Note that Figure B-2 shows the PID-controller outputs for $Sim_{H_{\infty,10MW}}$.

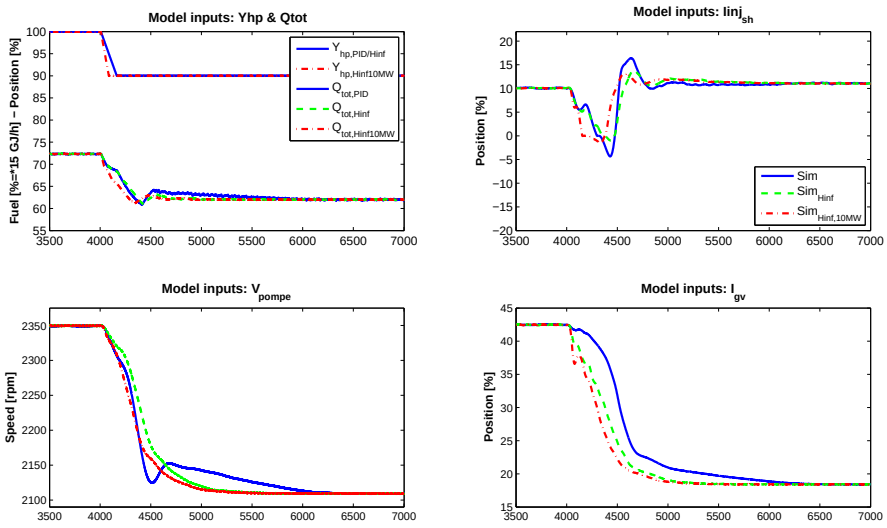

Figure B-2: PID-control signals in $Sim_{H_{\infty,10MW}}$

B-2 H_∞ Control Signals

During simulation of the $Charge_{ref}$-change scenario the H_∞-controllers (in Sim_{H_∞} and $Sim_{H_{\infty,10MW}}$) generate control signals Δy_{ref} (as shown in Figure 1-4). For input into the PID-controllers (see Figures), control signals Δy_{ref} are combined with original reference signals y_{ref} (hence $y_{ref} + y\Delta y_{ref}$). Figure B-3 shows the $y_{ref} + y\Delta y_{ref}$ that are generated in Sim_{H_∞} and $Sim_{H_{\infty,10MW}}$.

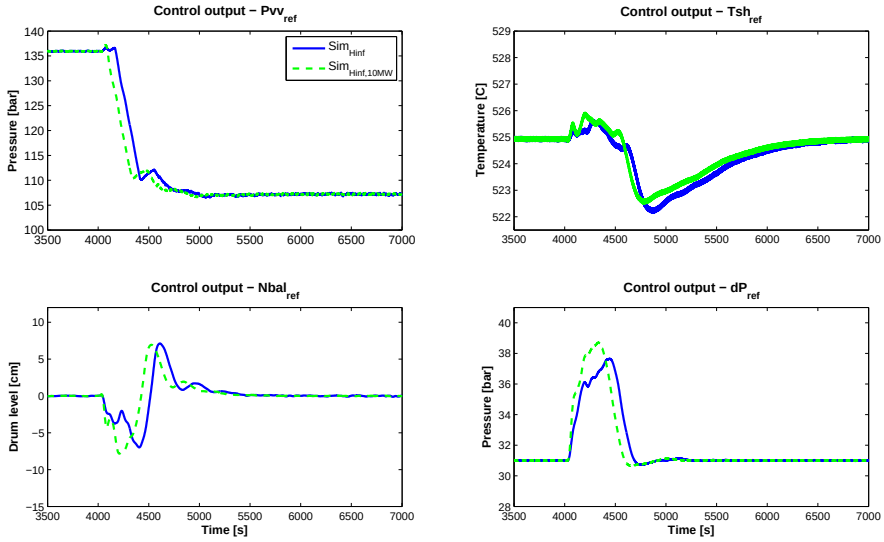

Figure B-3: Reference + H_∞-control-output signals, produced in Sim_{H_∞} and $Sim_{H_{\infty,10MW}}$

Figure B-3 does not show strange behavior.Furthermore, the H_∞-controller takes only small actions to govern the process. Note that the original references for Tsh, $Nbal$ and dP are constant values: resp. $525°C$, $0cm$ and $31bar$. Pvv_{ref} is calculated per situation by the Pressure Setpoint Calculation module.

B-3 Response Analysis Definitions

Throughout the study responses are analyzed using the following terms:

- Overshoot.
- Settling time.
- Fall time

The definition of these terms is inspired on the definitions used in [19]. The terms are defined as follows:

Overshoot (M_p)
Overshoot is measured in as the oscillation amplitude, which is given by the lowest peak amplitude + highest peak amplitude.

Settling time (t_s)
Settling time is measured by a band around the steady state value. The band is defined is defined as follows:

$Charge$ and Pvv	=	1%
Tsh	=	$0.2°C$
$Nbal$	=	$0.1cm$
dP	=	$0.2bar$

These values have been calculated by analysing the response of Sim (see Figure 2-3), near these values the process seems settled.

Rise time (t_r)
The rise time is measured as the time between 10% and 90% of the change in reference value (for scenario 3, $32MW$ and $29bar$). Rise time is only considered for $Charge$ and Pvv.

Appendix C

Power plants

C-1 About Power Plants

Power plants have been supplying power for industrial use since the late 1880s. Since this time several power plant types have been developed, varying in fuel, thermodynamic principle and design. However, all power plants have one concept in common: power is produced by conversion of heat to rotation.

In most power plants this conversion is achieved through a relatively simple water-steam cycle. The cycle consists of four steps; fist cold water is compressed. Then it is heated to steam. Thereafter steam is expanded in a turbine (rotation). And finally the steam is cooled and turns into water.

In most power plants the required heat is produced in a boiler by combustion of fossil fuel. The boiler consists of a furnace, flue gas heat exchangers and a drum. The furnace wall is made up of evaporator pipes. Through these pipes water absorbs heat and locally turns into steam, a water-steam mixture results. The water-steam mixture flows into the drum, a tank where the mixture separates naturally. On their way to the exhaust / stack, the hot (flue) gasses pass a set of heat exchangers. These heat exchangers remove as much energy as possible.

A drum is the center of the boiler. It serves as supply of hot water and steam for the entire boiler. Hot water, coming from the economizer, enters the drum. This water flows by itself into the evaporator pipes. This principle is called natural circulation. By density difference the water-steam mixture flows by itself back into the drum and separates. Steam collects at the top of the drum and hot water stays below.

After the furnace, the gasses contain still a large amount of heat. As it would be a waste to leave the heat unutilized, the flue gas is guided through a set of heat exchangers. The first set is called super heaters. In the super heater steam, from the drum, is heated far above evaporation temperatures (super heating). Temperatures reach up to as much of 500 deg C. The flue gas heat exchangers are arranged by heat consumption, hence the high temperature heaters are placed close to the furnace and the lowest temperature heater is near the exhaust. The lowest temperature heat exchanger is called economizer, and is used to heat the compressed water as much as possible before it enters the drum.

Steam, of correct conditions (pressure, temperature and flow), flows into the turbine, where it has space to expand. During expansion high velocity steam flows past turbine blades, pushing them to rotation. This creates a rotating force, which is transferred to the power (electricity) generator by turbine shaft. Hence power is produced.

After the turbine, low energy steam is left. To turn steam into cold water, the heat is removed in an externally cooled heat exchanger (condenser). Thereafter, water is stored in the feedwater tank. As this is a continuous process, at the same time water is drawn from the tank by the feed pump.

The feed pump presses a certain water flow through the opening of the boiler valve. This creates the desired water pressure. A series of heat exchangers, fed with waste steam of the turbine, increase the water temperature as much as possible. Finally hot water enters the boiler through the economizer.

C-2 Power Plant Control

It is impossible to operate such a large group of complex apparatuses without some sort of control system. Synchronized operation and achievement of the desired result, the required power production, is a complex control problem. To assure correct operation, many process variables (temperature, pressure, flow) are to be regulated.

The main objective of power plant control system is achievement of the desired power output by the power plant. Furthermore the control system is responsible for correct operation of many components and even more variables. Moreover, to achieve the desired production all components have to operate as one; the control system should harmonize operation. Finally the outside world requires a safe and reliable power supply, therefore a power plant control system should be reliable, safe, easy adjustable and intuitive.

Coordinated Control System

To fulfill these requirements conventional power plant are equipped with the Coordinated Control (CC) system. The CC-system is a multi-layered single input single output (SISO) PI and PID control system. As the name suggests, the CC-system coordinates the control of all components in the power plant. Through a clever choice of structure and controlled variables, the CC-system allows control of many components as if they are stand-alone. In fact this structure enables to control relatively complex components through basic PI(D) control.

As discussed in last section, power output is the result of expansion of steam in the turbine. Hence, the properties of the steam, e.g. pressure, temperature and flow, are the only factor influencing the power output. The structure of the CC-system is based on this principle. In other words, Coordinated Control achieves the required power production through control of steam properties, and more specific the steam flow to the turbine and the steam pressure in the boiler.

The CC-system calculates the required steam flow to achieve a certain specified output. Resulting data is passed on to the turbine controller, which uses this to regulate the steam flow by valve. This is a very fast method since opening and closing the valve is only a matter of seconds. Hence turbine control allows fast response to power demand changes.

However, the available amount of steam is limited (drum). Therefore, turbine control is only used as short-term power regulation. The aim is to give the boiler just enough time to adapt the steam production. Moreover, turbine control can also be used for disturbance rejection in the power output. By fast actuation of the turbine valve the power output can be smoothed.

While the turbine controller provides a fast response by regulation of the steam flow, the pressure inside the boiler changes. The boiler pressure controller measures it and calculates the required fuel flow to compensate it. However, due to the size of the boiler the response is slow. Hence the drum is used as steam buffer.

Taken together, Coordinated Control allows the control of the turbine and boiler as if they were stand-alone. Furthermore, due to the structure a very elegant method is found to combine and control a slow (boiler) with a fast system (turbine). Moreover, by reasoning from power output and demand, the CC-system directly addresses two of the three essential steam properties.

Feedwater (control) System

As the steam consumption (turbine) and production (boiler) are influenced by a change in the power demand, the water level in the drum also changes. The level of water in the drum is a measure for how much water is consumed for steam generation in the boiler. Based on the water level in the drum, the feed pump is regulated to produce the required water flow.

Work of the feed pump creates a water flow with a certain pressure. The pressure output is a result of the pump characteristic and works through the entire boiler; hence it also influences the steam outlet pressure.

In order to prevent disturbance of the steam outlet pressure, evaporation and cooling a form of compensation is required. To this aim, directly after the pump, a valve is placed: the boiler valve. By measuring the pressure difference between the feed pump outlet and the pressure in the drum, the valve position is regulated.

Again through the clever selection of control structure and variables, the control in the feedwater system can be done with basic PI(D) controllers. Furthermore, feedwater control is an essential aspect of the steam outlet condition control and the steam pressure specifically.

Temperature Control
After the drum, steam flows directly into the super heater absorbing as much of the provided heat as possible. Hence to achieve the desired steam outlet temperature some form of control is required. Moreover, without control the temperatures could become too high, possibly resulting in overheating and damage of the heat exchangers. Therefore each super heater is equipped with a cooling control system.

The cooling system consists of a cold-water injector and a master-slave PID control system. This system receives cold water directly from the feed pump. The temperature and the required cooling is achieved through actuation of a control of a valve. Opening of the valve allows a certain flow of cold water to be directly injected into the super heater.

C-3 Effect of settling time and oscillation amplitude on overall efficiency

In Chapter 3 is shown that H_∞-control reduces oscillation amplitude of the boiler outlet steam temperature with $1.5°C$ (i.e. a 15% reduction for this loop). Compared to the other results this is small decrease (e.g. in other loops amplitude is reduced with more than 70%). However, this decrease allows power plant operators to raise the boiler outlet steam temperature reference (i.e. Tsh_{ref}) with the same $1.5°C$.

Again this is not a big increase. Its influence on fuel costs however is not small, especially when considering large power plants. This becomes clear when calculating the difference in fuel consumption (i.e. fuel costs) for different sizes of power plants (e.g. power output: 135, 250, 500 and $1000MWe$) with and without H_∞-control.

First, the overall efficiency of a conventional (i.e. PID-controlled) and a H_∞-controlled power plant (i.e. with the higher Tsh_{ref}) are calculated. The difference between the two indicates the influence of the higher Tsh_{ref}. Overall efficiency is calculated using Carnot [10] (also see 'Why use Carnot').

$$\eta = 1 - \frac{T_l}{T_h} \tag{C-1}$$

Where:
T_l lowest system temperature.
T_h highest system temperature.
Considering the TS-diagram (please refer to [10]) of a typical power plant it is clear that the lowest system temperature is found at the condenser outlet ($20°C$). We assume that this value is equal in both the PID- and H_∞-controlled power plant. The highest system temperature is found at the boiler outlet. For the PID-controlled power plant the boiler outlet steam temperature is $525°C$ and, as mentioned earlier, for the H_∞-controlled plant it is $1.5°C$ higher. For clarity the values are presented in Table C-1.

	Description	PID $[°C]$	H_∞ $[°C]$
T_l	temperature at the condenser outlet	20	20
T_h	boiler outlet steam temperature	525	526.5

Table C-1: System temperatures in initial and H_∞-controlled power plant

With these values the overall efficiency of the conventional power plant is: $\eta_{PID} = 63.27\%$. The efficiency of the H_∞-controlled power plant is: $\eta_{H_\infty} = 63.34\%$. Note that in practice the overall efficiency is much lower (about 34%).

To produce 135, 250, 500 and $1000MWe$ in a conventional or a H_∞-controlled power plant requires a certain amount of input power (i.e. thermal energy). The amount of input power depends on resp η_{PID} and η_{H_∞}. The required input power of the two types is calculated with Equation C-2.

$$IP = \frac{OP}{\eta} \tag{C-2}$$

Where:
IP Input power $[MW]$.
OP Output power $[MW$, i.e. $MWe]$.
Subtracting the input power of the two plant types (i.e. PID- and H_∞-controlled) for each size indicates the difference in energy consumption due to the increased Tsh_{ref}. The following results are obtained (see Table C-2):

OP $[MW]$	IP_{PID}	IP_{H_∞}	Δ Power $[MW]$	Δ Fuel $[tons/year]$
135	213.36	213.13	0.2321	162.6
250	395.12	394.69	0.4298	301.2
500	790.24	789.38	0.8596	602.4
1000	1580.5	1578.8	1.7191	1204.8

Table C-2: Energy consumption of initial and H_∞-controlled power plant

Assuming a certain fuel type (e.g. fuel oil, methane or coal) and price, the difference in energy consumption can be translated into fuel costs for a certain period. Suppose both plants are fired with fuel oil (price: $327.52Euro/ton$; heating value: $45MJ/kg$), the following difference in fuel costs are found (see Table C-3).

Output power $[MW]$	Δ Fuel Cost $[Euro/year]$
135	53.270
250	98.650
500	197.290
1000	394.590

Table C-3: Fuel cost reduction by H_∞-control

Why use Carnot

Carnot provides a useful method to calculate the influence of different temperatures on overall efficiency. We reason it is allowed to use Carnot since we are more interested in the efficiency difference than the actual value. Other methods can be used to calculate overall efficiency and probably give much lower values for both power plant types. However, the in- or decrease, caused by the higher temperature, is probably the same.

Bibliography

[1] G. Oluwande, "Exploitation of advanced control techniques in power generation," *Computing and Control Engineering Journal*, vol. 12, pp. 63–7, 2001.

[2] G. Poncia and S. Bittanti, "Multivariable model predictive control of a thermal power plant with built-in classical regulation," *International Journal of Control*, vol. 74, no. 11, pp. 1118–1130, 2001.

[3] M. Cregan and D. Flyn, *Thermal power plant simulation and control*, ch. 1.

[4] S. Skogestad and I. Postlethwaite, *Multivariable Feedback Control: Analysis and Design*. John Wiley and Sons, Ltd, 2005.

[5] R. Dolezal and L. Varcop, *Process dynamics automatic control of steam generation plant*. Elsevier, 1970.

[6] G. Klefenz, *Automatic control of steam power plants*. Bibliographisches Institut, 1971.

[7] E. Wictor, "Multivariable feed water control for an electrical power plant," Master's thesis, Delft University of Technology, 2007.

[8] D. V. Massenhove, "Conception d'un simulateur de centrale électrique basé sur la physique du processus et identification de modèles boîtes noires en vue du développment de régulations predictives multivariables," Master's thesis, Université Catholique de Louvain, 2003.

[9] R. Garduno-Ramirez and K. Lee, "Intelligent hybrid coordinated-control of fossil fuel power units," *Proc. International Conference on Intelligent System Applications to Power Systems*, pp. 177–182, June 2001.

[10] H. S. M.J. Moran, *Fundamentals of Engineering Thermodynamics*. John Wiley and Sons, Ltd, 1998.

[11] S. Cambier, "Modelisation du fonctionnement dynamique d'une turbine à vapeur à soutirages et resurchauffe en vue de son intégration dans un simulateur de centrale électrique classique," Master's thesis, Université Catholique de Louvain, 2006.

[12] G. G. V. Wertz, E. Silva and B. Codrons, "Performance limitations arising in the control of power plants," *The International Federation of Automatic Control*, July 2008.

[13] C. Garcia and M. Morari, "Internal model control: A unifying review and some new results," *Ind. Eng. Chem. Process Dev.*, vol. 2, no. 21, pp. 308–323, 1982.

[14] D. C. McFarlane and K. Glover, "Robust stabilization of normalized coprime factor plant descriptions with h_∞ bounded uncertainty," *IEEE Transactions on Automatic Control*, no. 38, pp. 821–830, 1989.

[15] MathWorks, *Matlab R2008b: Help.* The MathWorks Inc., 2008.

[16] P. M. J. van den Hof, *System Identification (reader).* Delft University of Technology, 2006.

[17] J. Doyle, "Synthesis of robust controllers and filters," *Proceedings of the IEEE Conference on Decision and Control*, vol. 1, pp. 109–114, Dec. 1983.

[18] P. K. J. Doyle, K. Glover and B. Francis, "State-space solutions to standard h_2 and h_∞ control problems," *IEEE Trans. Automat. Contr.*, vol. AC-34, pp. 831–847, Aug. 2006.

[19] J. P. G.F. Franklin and A. Emami-Naeini, *Feedback Control of Dynamic Systems.* Prentice Hall, 2002.